RadioGraphics

# Eosinophilic Lung Diseases: A Clinical, Radiologic, and Pathologic Overview[1]

*Yeon Joo Jeong, MD • Kun-Il Kim, MD • Im Jeong Seo, MD • Chang Hun Lee, MD • Ki Nam Lee, MD • Ki Nam Kim, MD • Jeung Sook Kim, MD Woon Jung Kwon, MD*

**CME FEATURE**

*See accompanying test at http://www.rsna.org/education/rg_cme.html*

**LEARNING OBJECTIVES FOR TEST 2**

*After reading this article and taking the test, the reader will be able to:*

- Describe the diagnostic criteria for and classification of eosinophilic lung diseases.
- Identify the clinical, pathologic, and radiologic findings in these diseases.
- Discuss the differential diagnoses for these diseases in terms of the pattern and distribution of abnormalities seen at thin-section CT.

**TEACHING POINTS**

*See last page*

Eosinophilic lung diseases are a diverse group of pulmonary disorders associated with peripheral or tissue eosinophilia. They are classified as eosinophilic lung diseases of unknown cause (simple pulmonary eosinophilia [SPE], acute eosinophilic pneumonia [AEP], chronic eosinophilic pneumonia [CEP], idiopathic hypereosinophilic syndrome [IHS]), eosinophilic lung diseases of known cause (allergic bronchopulmonary aspergillosis [ABPA], bronchocentric granulomatosis [BG], parasitic infections, drug reactions), and eosinophilic vasculitis (allergic angiitis, granulomatosis [Churg-Strauss syndrome]). The percentages of eosinophils in peripheral blood and bronchoalveolar lavage fluid are essential parts of the evaluation. Chest computed tomography (CT) demonstrates a more characteristic pattern and distribution of parenchymal opacities than does conventional chest radiography. At CT, SPE and IHS are characterized by single or multiple nodules with a surrounding ground-glass-opacity halo, AEP mimics radiologically hydrostatic pulmonary edema, and CEP is characterized by nonsegmental airspace consolidations with peripheral predominance. ABPA manifests with bilateral central bronchiectasis with or without mucoid impaction. The CT manifestations of BG are nonspecific and consist of a focal mass or lobar consolidation with atelectasis. The most common CT findings in Churg-Strauss syndrome include subpleural consolidation with lobular distribution, centrilobular nodules, bronchial wall thickening, and interlobular septal thickening. The integration of clinical, radiologic, and pathologic findings facilitates the initial and differential diagnoses of various eosinophilic lung diseases.



**Abbreviations:** ABPA = allergic bronchopulmonary aspergillosis, AEP = acute eosinophilic pneumonia, BAL = bronchoalveolar lavage, BG = bronchocentric granulomatosis, CEP = chronic eosinophilic pneumonia, DRESS = drug rash with eosinophilia and systemic symptoms, FDG = 2-[fluorine-18]fluoro-2-deoxy-D-glucose, H-E = hematoxylin-eosin, IHS = idiopathic hypereosinophilic syndrome, PP = pleuropulmonary paragonimiasis, SPE = simple pulmonary eosinophilia

**RadioGraphics 2007;** 27:617–639 • **Published online** 10.1148/rg.273065051 • **Content Codes:** CH CT

[1]From the Departments of Diagnostic Radiology (Y.J.J., K.-I.K., I.J.S.) and Pathology (C.H.L.), Pusan National University Hospital, Pusan National University School of Medicine and Medical Research Institute, 1-10, Ami-Dong, Seo-gu, Pusan 602-739, Korea; the Department of Radiology, Dong A University Hospital, Pusan, Korea (K.N.L., K.N.K.); the Department of Radiology, Dongguk University International Hospital, Gyeonggi-do, Korea (J.S.K.); and the Department of Radiology, Ulsan University Hospital, Ulsan, Korea (W.J.K.). Recipient of a Certificate of Merit award for an education exhibit at the 2005 RSNA Annual Meeting. Received April 3, 2006; revision requested May 3; final revision received August 21; accepted August 22. All authors have no financial relationships to disclose. **Address correspondence to** Y.J.J. (e-mail: *lunar9052@hanmail.net*).

See the commentary by Frankel et al following this article.

**Table 1**
**Classification of Eosinophilic Lung Diseases**

| |
|---|
| Eosinophilic lung diseases of unknown cause |
| SPE |
| AEP |
| CEP |
| IHS |
| Eosinophilic lung diseases of known cause |
| ABPA |
| BG |
| Parasitic infections |
| Drug reactions |
| Eosinophilic vasculitis |
| Allergic angiitis |
| Granulomatosis (Churg-Strauss syndrome) |

## Introduction

Eosinophilic lung diseases are a diverse group of disorders characterized by pulmonary opacities associated with tissue or peripheral eosinophilia. The diagnosis of eosinophilic lung disease can be made if any of the following findings is present: *(a)* pulmonary opacities with peripheral eosinophilia, *(b)* tissue eosinophilia confirmed at either open or transbronchial lung biopsy, or *(c)* increased eosinophils in bronchoalveolar lavage (BAL) fluid (1). A large variety of pulmonary diseases may be associated with occasional blood eosinophilia of a minor degree. These diseases include asthma; various pulmonary infections such as coccidioidomycosis, *Pneumocystis jirovecii* infection, and mycobacteria; some types of tumor (eg, non–small cell lung carcinoma, lymphoma, lymphocytic leukemia); collagen vascular disorders such as rheumatoid disease and Wegener granulomatosis; idiopathic pulmonary fibrosis; and Langerhans cell histiocytosis (2–6). However, these conditions are not usually considered to be eosinophilic lung diseases, in which a tissue eosinophilia is by definition pathogenically significant.

The eosinophil is a polymorphonuclear leukocyte containing several eosinophil-specific proteins in cytoplasmic granules (Fig 1). An eosinophil can serve as an end-stage effector cell but can also have specialized roles in the host defense mechanism. However, the eosinophil sometimes harms the host by releasing specific proteins that are potentially cytotoxic to tissues, resulting in pathologic processes (7). One of these proteins is the protein that forms Charcot-Leyden crystals, the bipyramidal crystals whose presence in sputum and tissues is a hallmark of eosinophil-related disease.

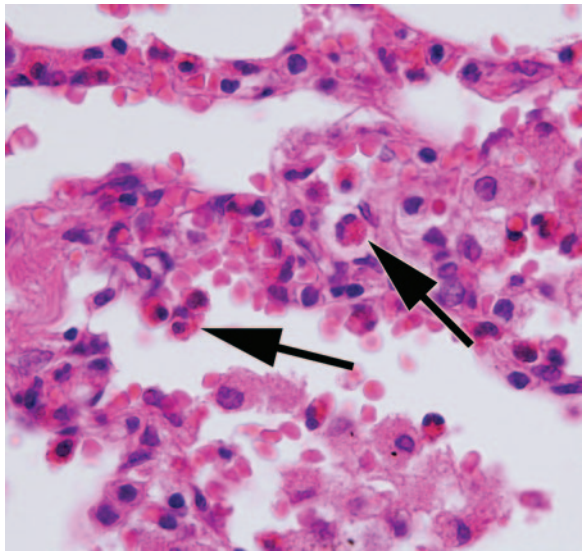

**Figure 1.** High-power photomicrograph (original magnification, ×1000; hematoxylin-eosin [H-E] stain) shows numerous eosinophils (arrows), each of which has a lobulated nucleus and cytoplasm that includes specific granules.

Teaching Point

Eosinophilic lung diseases are generally classified as those of unknown cause (simple pulmonary eosinophilia [SPE], acute eosinophilic pneumonia [AEP], chronic eosinophilic pneumonia [CEP], idiopathic hypereosinophilic syndrome [IHS]) and those of known cause (allergic bronchopulmonary aspergillosis [ABPA], bronchocentric granulomatosis [BG], parasitic infection, drug reaction), as well as eosinophilic vasculitis (allergic angiitis, granulomatosis) (Table 1). Some eosinophilic lung diseases are predominantly airway based, whereas others are parenchymal or a mixture of both. A new disease entity known as eosinophilic bronchiolitis, which is characterized by pathologic and radiologic findings that suggest eosinophilic bronchiolar involvement, has been reported (8).

In this article, we discuss and illustrate the general diagnostic approach to and the characteristic clinical, histologic, and radiologic findings in the various eosinophilic lung diseases.

## Diagnostic Methods

The most valuable clinical information is derived from the patient's history and from physical examination. The duration and severity of symptoms are also of critical importance. A history of asthma may raise suspicion for Churg-Strauss syndrome, ABPA, or BG. Travel history may suggest parasitic infection. A careful history of the use of prescription and illicit drugs should be obtained.

A white blood cell differential count is an essential part of the evaluation of eosinophilic lung

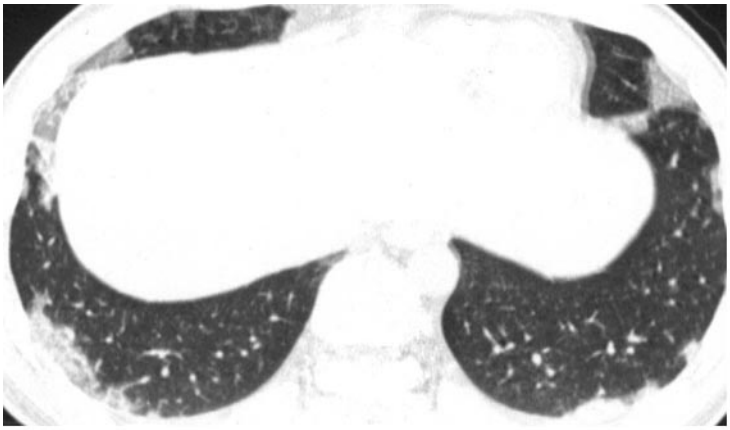

2.

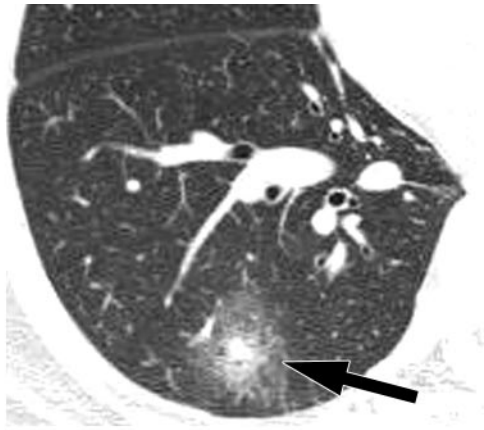

3.

**Figures 2, 3.** **(2)** SPE in a 25-year-old man with 13.5% peripheral eosinophilia. Transverse thin-section (1-mm collimation) CT scan (lung windowing) shows consolidation and ground-glass opacity involving mainly the peripheral regions of both lower lobes. At follow-up radiography performed 10 days later, the parenchymal opacities had cleared spontaneously. **(3)** SPE in a 46-year-old woman with 30.1% peripheral eosinophilia. Transverse thin-section (1-mm collimation) CT scan (lung windowing) shows an airspace nodule with surrounding ground-glass opacity in the right lower lobe (arrow). At follow-up chest radiography, the nodule had disappeared.

disease. Although several different normal values have been reported, normal blood generally contains 50–250 eosinophils per microliter (1). Most eosinophilic lung diseases manifest with peripheral eosinophilia, although AEP may not. Stool examination and serologic testing are helpful in evaluating patients with specific conditions such as parasitic infection and ABPA.

Pulmonary function tests can occasionally be useful in the evaluation of patients with unexplained pulmonary eosinophilia. Some eosinophilic lung diseases (AEP, CEP, tropical pulmonary eosinophilia) are typically accompanied by mainly restrictive ventilatory defects, whereas others (ABPA, Churg-Strauss syndrome) typically cause mainly obstructive ventilatory defects.

BAL can also be very useful in the evaluation of patients with eosinophilic lung disease. Normal BAL fluid consists of less than 1% eosinophils. Because some disorders are not accompanied by peripheral eosinophilia, BAL may provide the first (and, perhaps, the only) indication of an eosinophilic lung disease.

Patients with eosinophilic lung disease may be identified initially on the basis of pulmonary symptoms or chest radiographic abnormalities accompanied by blood or tissue eosinophilia. Diverse and nonspecific findings may also be seen at conventional chest radiography. Chest computed tomography (CT) demonstrates a more characteristic pattern and distribution of parenchymal opacities than does chest radiography. Although the characteristic CT findings are often helpful, there is still a considerable overlap of CT findings among the various eosinophilic lung diseases (9).

Open lung biopsy may be necessary to confirm diseases such as Churg-Strauss syndrome and BG. Biopsy is generally not required for the diagnosis of ABPA, IHS, drug reactions, or parasitic infections.

## Eosinophilic Lung Diseases of Unknown Cause

### Simple Pulmonary Eosinophilia

SPE, or Loeffler syndrome, was originally reported as a benign AEP of unknown cause characterized by migrating pulmonary opacities, increased peripheral blood eosinophils, minimal or no pulmonary symptoms, and spontaneous resolution within 1 month. In some patients, these clinical characteristics may prove to be secondary to the presence of parasites, ABPA, or drugs (10,11). Pathologic specimens show edema and accumulation of eosinophils in the alveolar septa and interstitium (1).

The radiographic manifestations of SPE consist of transient and migratory areas of consolidation that typically clear spontaneously within 1 month (12). These consolidations are nonsegmental, may be single or multiple, usually have ill-defined margins, and often have a predominantly peripheral distribution (1,12). High-resolution CT findings consist of ground-glass opacity or airspace consolidation involving mainly the peripheral regions of the middle and upper lung zones (Fig 2) (9), as well as single or multiple airspace nodules with surrounding ground-glass opacity (Fig 3) (9,13). The differential diagnosis

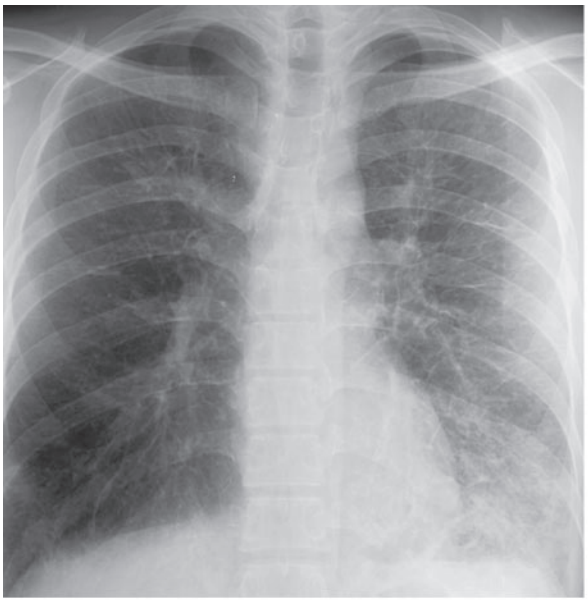

4a.

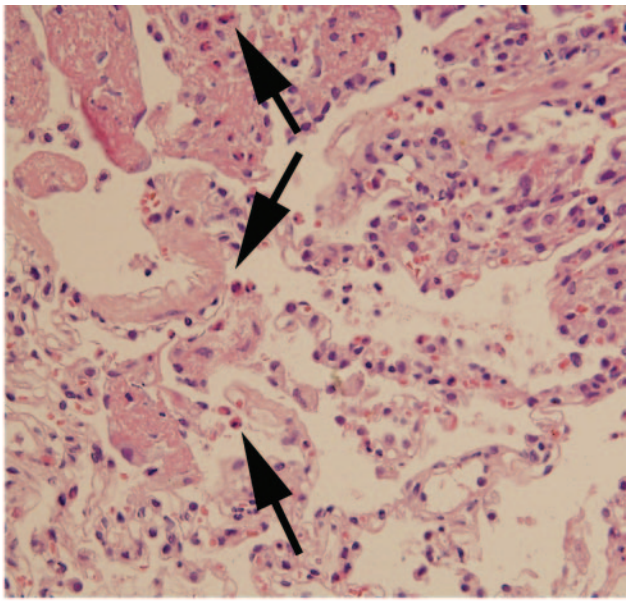

4c.

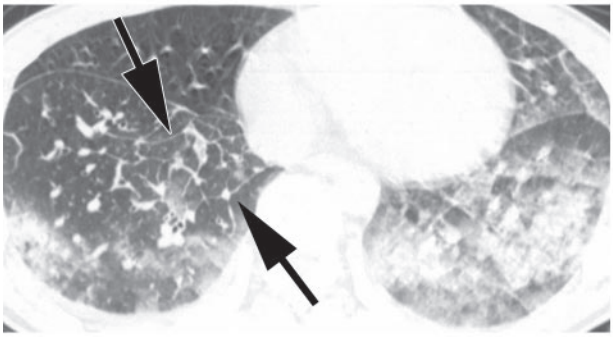

4b.

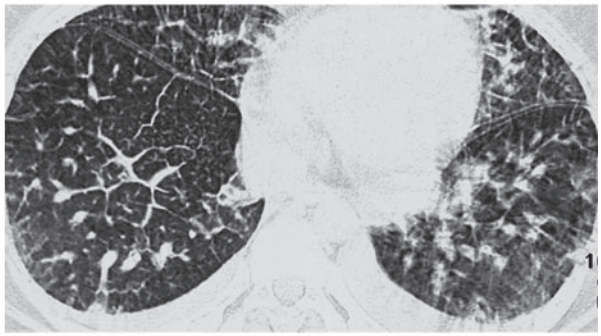

5.

**Figures 4, 5.** **(4)** AEP in a 29-year-old man with 26% BAL fluid eosinophilia. **(a)** Chest radiograph obtained 7 days after the onset of dyspnea reveals reticular densities with patchy consolidation and ground-glass opacities in both lungs. **(b)** Thin-section (1-mm collimation) CT scan (lung windowing) shows multifocal patchy areas of ground-glass opacity and consolidation with smooth interlobular septal thickening (arrows) in both lower lobes. Bilateral pleural effusions are also seen. **(c)** High-power photomicrograph (original magnification, ×400; H-E stain) of a transbronchial lung biopsy specimen obtained from the left lower lobe 5 days after **a** shows the infiltration of eosinophils (arrows) and lymphocytes into the alveolar spaces and alveolar walls. Note the absence of interstitial fibrosis. **(5)** AEP in an 18-year-old woman with acute onset of fever and dyspnea. The patient had 27% BAL fluid eosinophilia. Thin-section (1-mm collimation) CT scan (lung windowing) shows areas of ground-glass opacity and interlobular septal thickening in both lungs. Bilateral pleural effusions are also seen.

for migratory pulmonary opacities includes pulmonary hemorrhage, pulmonary vasculitis, cryptogenic organizing pneumonia, and recurrent aspiration. In patients with airspace nodules with a ground-glass-opacity halo, the differential diagnosis includes both infectious diseases (invasive pulmonary aspergillosis, mucormycosis, candidiasis) and noninfectious diseases (Wegener granulomatosis, primary and metastatic hemorrhagic tumors, bronchioloalveolar carcinoma, pulmonary lymphoma) (14).

## Acute Eosinophilic Pneumonia

AEP represents a clinical entity that is distinct from other idiopathic eosinophilic lung diseases. Diagnostic criteria include acute febrile illness of less than 5 days' duration; hypoxemia; diffuse alveolar or mixed alveolar-interstitial opacities on chest radiographs; BAL fluid consisting of more than 25% eosinophils; absence of parasitic, fungal, or other infection; prompt and complete response to corticosteroids; and no relapse after discontinuation of corticosteroids. Peripheral blood eosinophil percentages are usually normal,

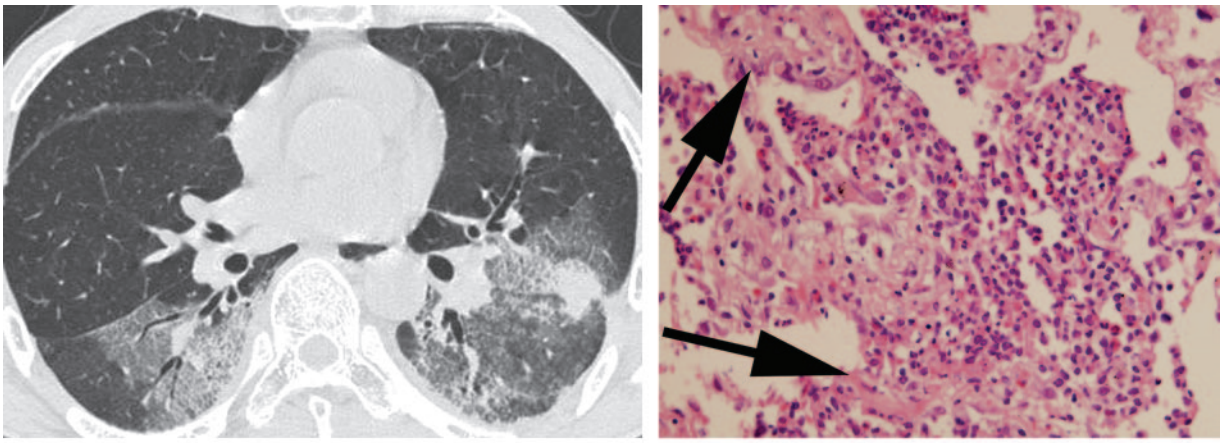

a. b.

**Figure 6.** CEP in a 59-year-old man with a 3-week history of severe cough and fever. The patient had 25% BAL fluid eosinophilia. **(a)** Thin-section (1-mm collimation) CT scan (lung windowing) shows ground-glass opacities with intralobular interstitial thickening in both lower lobes. **(b)** High-power photomicrograph (original magnification, ×400; H-E stain) of a transbronchial lung biopsy specimen shows infiltration of eosinophils and polymorphous inflammatory cells into the alveolar lumen and interstitium and a varying degree of interstitial fibrosis (arrows).

although they become elevated during the subsequent clinical course (1). Unlike with blood eosinophils, a very high percentage of BAL eosinophils is characteristic of AEP (15). Pulmonary function testing in the acute phase shows a restrictive pattern (16). Patients respond rapidly to high doses of corticosteroids, usually within 24–48 hours. Unlike patients with CEP, patients with AEP do not experience relapse after discontinuation of corticosteroids (16,17).

The cause of AEP remains unknown; however, AEP-like signs and symptoms have been reported after cigarette smoking (18,19) or exposure to dust (20) or smoke from fireworks (21).

The principal histologic finding in AEP is diffuse alveolar damage associated with interstitial and alveolar eosinophilia (Fig 4) (22).

The predominant radiographic findings in AEP are bilateral reticular densities (with or without areas of patchy consolidation) and pleural effusion (Fig 4) (23,24). The predominant patterns of parenchymal abnormality seen at CT are bilateral patchy areas of ground-glass opacity, frequently accompanied by interlobular septal thickening and sometimes by consolidation or poorly defined nodules (Figs 4, 5) (23,24).

The radiologic differential diagnosis for AEP includes hydrostatic pulmonary edema, adult respiratory distress syndrome or acute interstitial pneumonia, and atypical bacterial or viral pneumonia (23). Because initial peripheral blood eosinophil counts are usually normal, however, developing a clinicoradiologic differential diagnosis for AEP is often difficult.

## Chronic Eosinophilic Pneumonia

CEP is an idiopathic condition characterized by chronic and progressive clinical features and specific pathologic findings (25). The clinical manifestation is usually insidious, and the patient experiences symptoms for an average of 7.7 months before the diagnosis is made (26). Most patients are middle aged, and approximately 50% have asthma (27). Women are more frequently affected than men (25). Pulmonary function tests can be normal in mild cases but usually show restrictive defects (26).

Peripheral blood eosinophilia is usually mild or moderate but occasionally is severe (26). Increased serum IgE levels are seen in two-thirds of patients (28). The erythrocyte sedimentation rate is usually elevated (26), and peripheral blood thrombocytosis has also been reported (29). The percentage of eosinophils in the BAL fluid is very high (30).

Histologic examination typically shows accumulation of eosinophils and lymphocytes in the alveoli and interstitium, with interstitial fibrosis (Fig 6) (25,26,31). An organizing pneumonia pattern or an eosinophilic abscess may also be seen (31). The essential histologic differences between AEP and CEP are related to *(a)* the severity of damage to the basal lamina, and *(b)* the amount of subsequent intraluminal fibrosis (31).

The typical chest radiographic finding in CEP is nonsegmental peripheral airspace consolidation ("photographic negative shadow of pulmonary

**Figure 7.** CEP in a 29-year-old man with 27.5% peripheral and 30% BAL fluid eosinophilia. **(a)** Chest radiograph shows airspace consolidation confined mainly to the peripheral lung (photographic negative shadow of pulmonary edema). **(b)** Transverse thin-section (1-mm collimation) CT scan (lung windowing) also shows airspace consolidation primarily involving the peripheral lung.

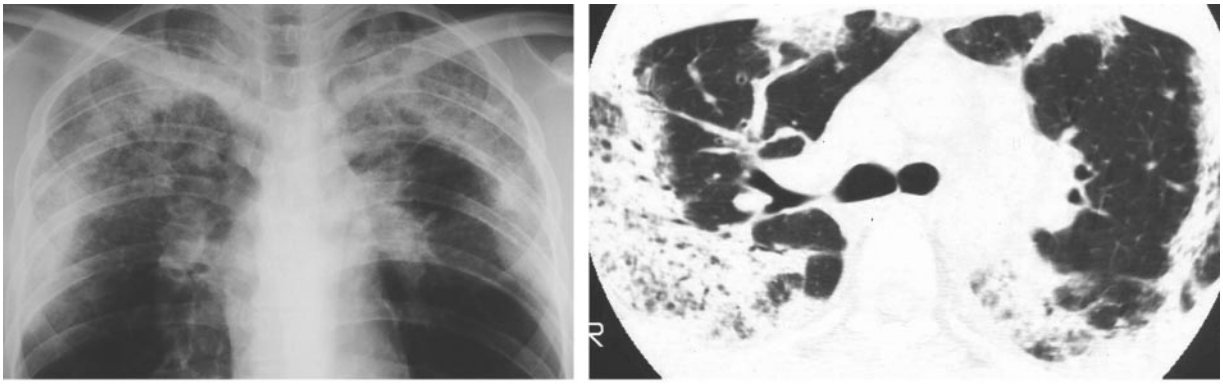

a. b.

edema") involving mainly the upper lobes (Fig 7) (25,32–34). However, this finding may be seen in less than 50% of cases (26). CT demonstrates typical nonsegmental areas of airspace consolidation with peripheral predominance (Fig 7) (33, 35). Less common findings include ground-glass opacities, nodules, and reticulation (Fig 6). These less common findings predominate in the later stages of CEP (33). CT performed more than 2 months after the onset of symptoms shows linear bandlike opacities parallel to the pleural surface (33). Pleural effusion is observed in less than 10% of cases (25,26,36).

A number of other conditions may mimic CEP at radiology, including bronchiolitis obliterans organizing pneumonia, Churg-Strauss syndrome, and Loeffler syndrome (35,37). Differentiation of Churg-Strauss syndrome from CEP is necessary in patients with peripheral eosinophilia and pulmonary abnormalities. At CT, CEP is characterized by the presence of homogeneous peripheral airspace consolidation, whereas in Churg-Strauss syndrome, peripheral consolidation has a tendency toward lobular distribution and, frequently, associated centrilobular nodules within the ground-glass opacity (37). The distribution of opacities is identical to that in Loeffler syndrome, although in the latter, the pulmonary opacities are transient and shift over days, whereas untreated CEP has a more protracted course (35).

Teaching Point

## Idiopathic Hypereosinophilic Syndrome

IHS is a rare disorder characterized by marked, prolonged idiopathic eosinophilia and by variable organ dysfunction related either to infiltration by eosinophils or secondarily to eosinophil-associated tissue damage (38). Diagnostic criteria include persistent eosinophilia of 1500 cells per cubic millimeter for more than 6 months or death within 6 months; the absence of parasitic, allergic, or other known causes of eosinophilia; and evidence of organ involvement and multiorgan system dysfunction (38,39). Onset usually occurs in the third or fourth decade of life, with a male-female ratio of 7:1 (40). The heart and central nervous system in particular are involved. Cardiac involvement, including endocardial fibrosis, restrictive cardiomyopathy, valvular damage, and mural thrombus formation, is the most significant complication of IHS (41). Pulmonary involvement occurs in up to 40% of patients. Most pulmonary involvement is related to cardiac failure leading to pulmonary edema. Thromboembolic disease; peripheral neuropathy; and involvement of the gastrointestinal tract, kidneys, joints, and skin have also been reported (40,42,43). The BAL fluid eosinophilia can be as high as 73% (38,44). Histopathologic analysis of IHS demonstrates striking eosinophilic infiltration of involved organs, including the lung, with associated disruption of the architecture and areas of necrosis (Fig 8) (39).

**Figure 8.** IHS in a 3-month-old boy with erythematous rash over his entire body. The patient had persistent eosinophilia of 1600 cells per cubic millimeter for 12 months. **(a)** Initial chest radiograph shows bilateral diffuse ground-glass opacities. **(b)** High-resolution CT scan obtained the same day shows diffuse ground-glass opacities in both lungs. **(c)** High-power photomicrograph (original magnification, ×400; H-E stain) of an open biopsy specimen obtained from the right lower lobe 1 month after **b** reveals infiltration of eosinophils into the alveoli and interstitium. Note the formation of indistinct granuloma (arrow). **(d)** High-power photomicrograph (original magnification, ×400; H-E stain) of a percutaneous liver biopsy specimen obtained 1 month after **b** reveals eosinophil infiltration into the sinusoids. Bone marrow biopsy revealed normocellular marrow consisting of 18% eosinophils and no blast cells. **(e, f)** CT scans (5-mm collimation, lung windowing) obtained 5 months after **b** show multiple nodules in the left upper lobe (arrows).

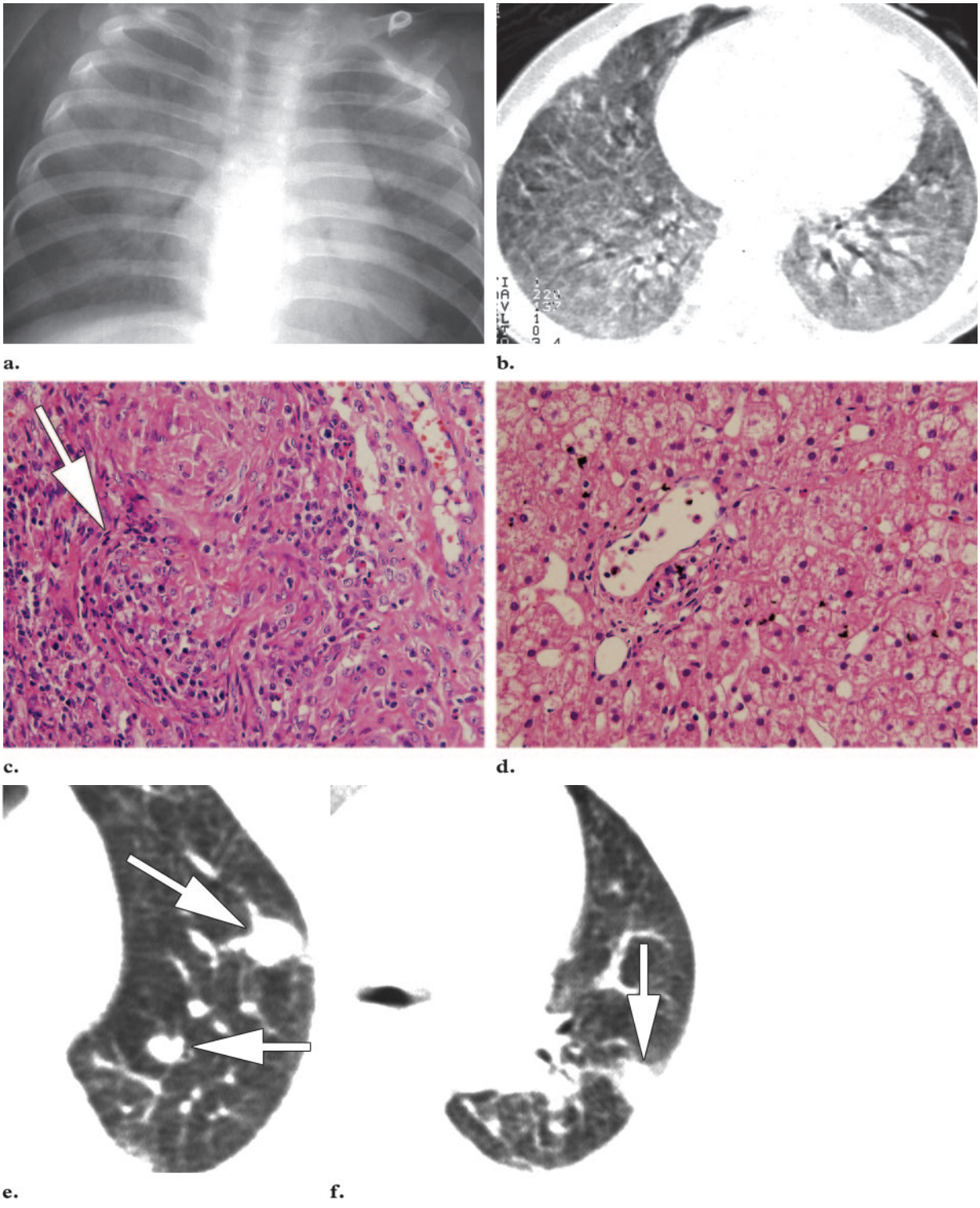

**Figure 9.** IHS in a 45-year-old man with persistent eosinophilia of 1800–3200 cells per cubic millimeter for more than 6 months. The patient had 52% BAL fluid eosinophilia. Transverse thin-section (1-mm collimation) CT scans (lung windowing) obtained at two levels reveal large nodules with surrounding ground-glass opacity in the left lung (arrow).

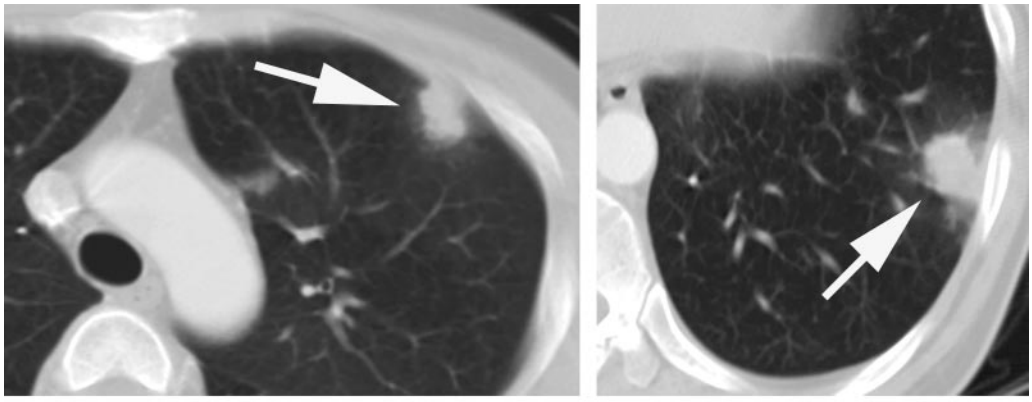

**a.** **b.**

Radiographic findings in IHS are often nonspecific and consist of focal or diffuse, interstitial or alveolar nonlobar opacities (38,39,44,45), with most pulmonary opacities being related to severe cardiac failure. Pleural effusion is seen in 50% of cases (38,39,44). CT shows nodules with or without surrounding ground-glass opacity and focal or diffuse areas of ground-glass opacity (Figs 8, 9) (13,46). The radiologic differential diagnosis for IHS is the same as that for Loeffler syndrome.

## Eosinophilic Lung Diseases of Known Cause

### Allergic Bronchopulmonary Aspergillosis

ABPA is a hypersensitivity reaction to *Aspergillus* antigens and is usually caused by *Aspergillus fumigatus*. ABPA is typically seen in patients with long-standing asthma or cystic fibrosis. It is believed that the *Aspergillus*-specific IgE-mediated type I hypersensitivity reaction and the specific IgG-mediated type III hypersensitivity reactions play an important role in the pathogenesis of ABPA (47).

ABPA is usually suspected on clinical grounds, and the diagnosis is confirmed at radiology and serologic testing (48). Diagnostic criteria include the presence of asthma, peripheral blood eosinophilia, an immediate positive skin test for *Aspergillus* antigens, increased serum IgE levels, and pulmonary opacity on chest radiographs. The IgE level is probably the most useful laboratory test for ABPA, since it correlates well with disease activity (49).

Because the diagnosis of ABPA is usually made on clinical grounds, lung biopsies are rarely performed for the diagnosis. In a study of 18 pathologic specimens obtained in patients with ABPA, the most significant findings involved the bronchi and bronchioles, with bronchocentric granulomas seen in 15 specimens and mucoid impaction in 11 (50). Other findings included granulomatous inflammation with histiocytes and lymphocytes, increased numbers of eosinophils, and exudative bronchiolitis (Fig 10). Fungal hyphae were commonly seen without evidence of tissue invasion (Fig 10) (50).

Patterson et al (51) divided ABPA into five stages to help guide the management of the disease: acute, remission, exacerbation, corticosteroid dependent, and fibrotic. Although radiographic findings may be normal, findings in early-stage disease typically include transient pulmonary opacities or homogeneous, tubular, gloved-finger areas of increased opacity in a bronchial distribution, usually either predominantly or exclusively involving the upper and central lungs (Fig 10a) (52–55). These opacities are related to the plugging of airways by hyphal masses with distal mucoid impaction. Occasionally, isolated lobar or segmental atelectasis may occur (56). In later stages, central bronchiectasis and pulmonary

**Figure 10.** ABPA in a 31-year-old asthmatic man with 15% peripheral eosinophilia. **(a)** Chest radiograph shows tubular and cystic lesions in the central portions of both lungs. Note also the mucus plugging with a gloved-finger appearance (arrows). **(b)** Thin-section (1-mm collimation) CT scan (lung windowing) demonstrates central bronchiectasis with mucus plugging (arrows), centrilobular nodules, and bronchial wall thickening involving predominantly the segmental and subsegmental bronchi of the upper lobes. **(c)** Photomicrograph (original magnification, ×100; H-E stain) of the impacted mucoid material from a bronchoscopic biopsy specimen reveals parallel rows of necrotic eosinophils and cellular debris within a mucinous background. **(d)** High-power photomicrograph (original magnification, ×400; Gomori methenamine silver stain) shows branching fungal hyphae within impacted mucus, a finding that is suggestive of *Aspergillus* species.

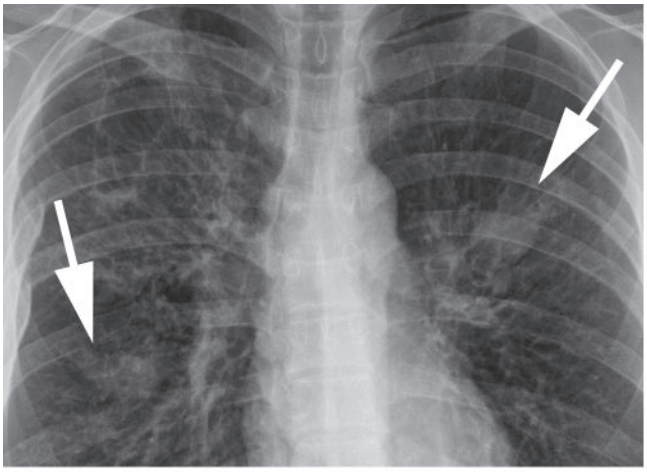

a.

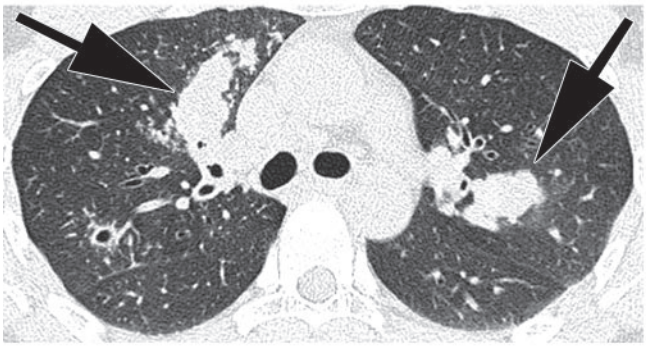

b.

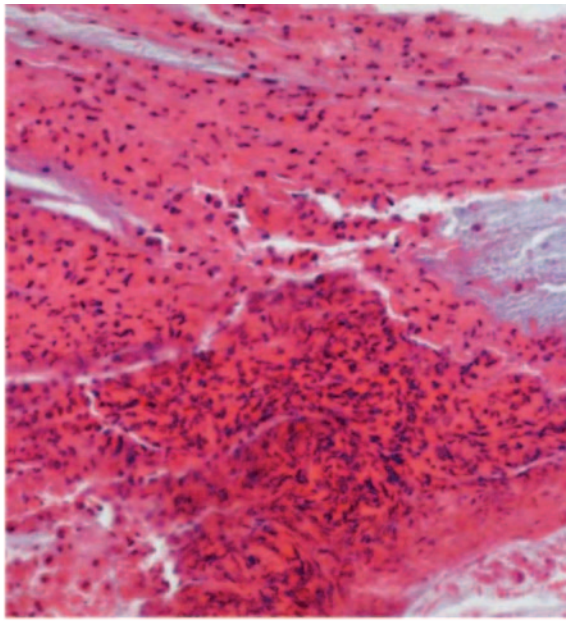

c.

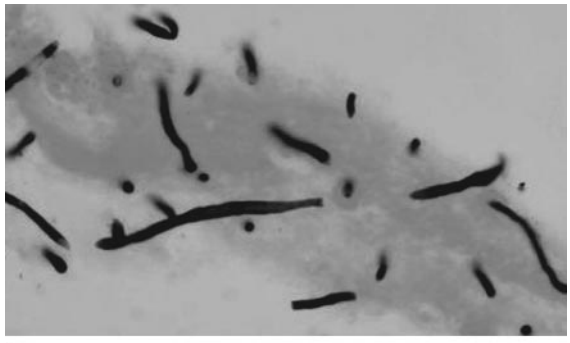

d.

fibrosis develop. CT findings in ABPA consist primarily of mucoid impaction and bronchiectasis involving predominantly the segmental and subsegmental bronchi of the upper lobes, along with centrilobular nodules or branching linear structures (Fig 10b) (54). In approximately 30% of patients, the impacted mucus is highly opaque or demonstrates frank calcification at CT (56). The differential diagnosis includes other causes of mucoid impaction such as endobronchial lesions, bronchial atresia, bronchiectasis, and bronchial asthma. Mild central bronchiectasis can be seen in asthma subsequent to chronic inflammation and does not necessarily indicate the presence of ABPA (54,57). However, in an asthmatic patient, ABPA is strongly suggested by the presence of randomly distributed, central, moderate to severe bronchiectasis predominantly involving the upper lungs; bronchial wall thickening; and centrilobular nodules (58).

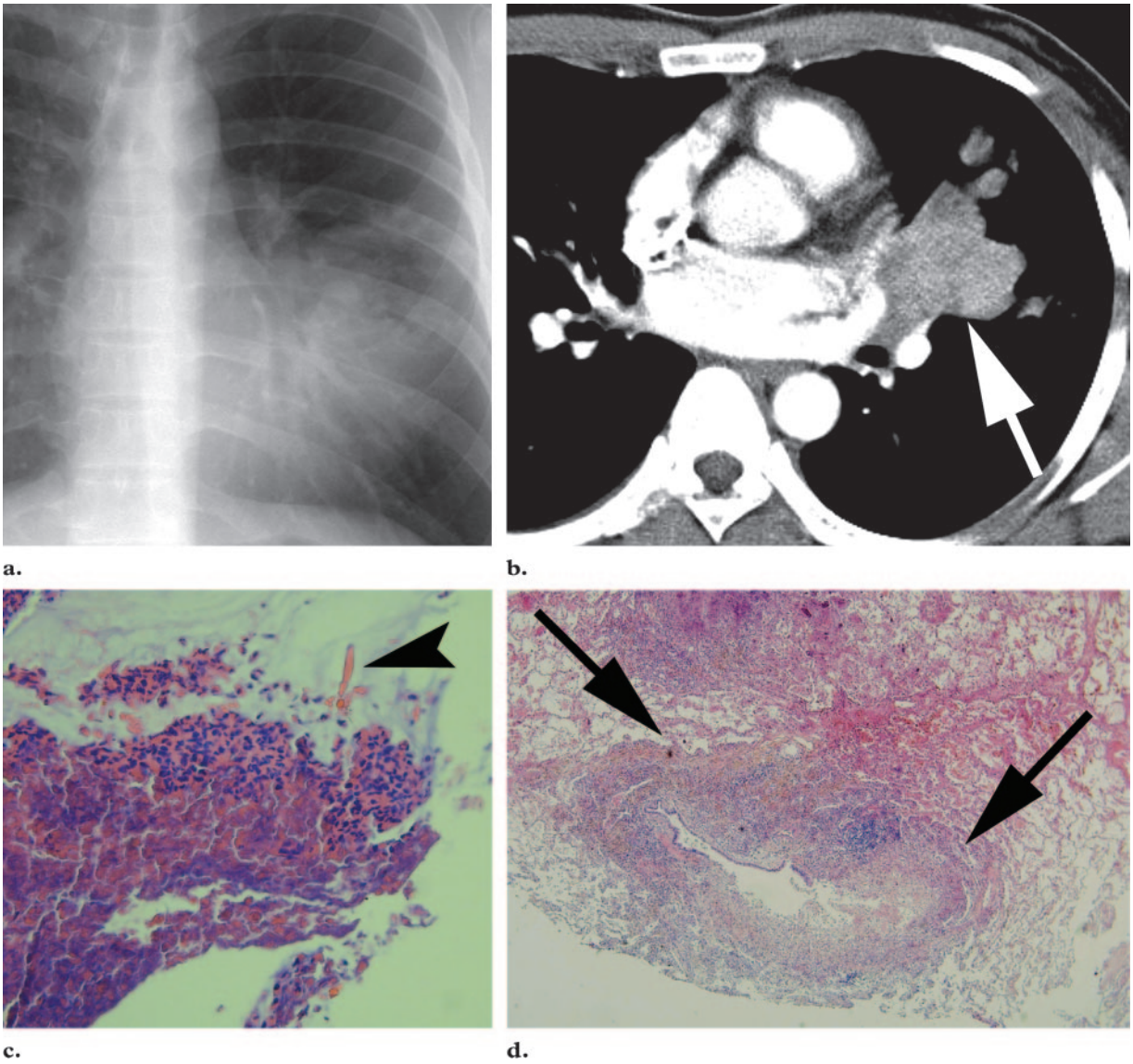


**Figure 11.** BG in a 25-year-old asthmatic man with 13% peripheral eosinophilia. **(a)** Chest radiograph shows consolidation and nodular opacities in the left upper lobe. **(b)** Transverse thin-section (2.5-mm collimation) CT scan (mediastinal windowing) obtained at the level of the left atrium shows a lobulated soft-tissue mass (arrow) with obstruction of the lingular segmental bronchus. **(c)** High-power photomicrograph (original magnification, ×400; H-E stain) of a bronchoscopic biopsy specimen shows eosinophilic cellular debris and Charcot-Leyden crystals (arrowhead). **(d)** Photomicrograph (original magnification, ×40; H-E stain) of the surgical specimen reveals bronchocentric granuloma formation (arrows) with focal necrosis.

## Bronchocentric Granulomatosis

BG is a rare disorder characterized by a necrotizing granulomatous inflammation of bronchial and bronchiolar epithelium with chronic inflammatory changes in the surrounding lung parenchyma (Fig 11) (59,60). Approximately one-third of affected patients have tissue eosinophilia and tend to have asthma, peripheral eosinophilia, fungal hyphae at biopsy, and positive sputum cultures for *Aspergillus* organisms (60,61). These patients may have a histologic component of ABPA. The remaining two-thirds of affected patients have neutrophils rather than eosinophils in the lung lesions (60,61) and do not have asthma. In nonasthmatic patients, the underlying cause of BG is often unclear.

The radiographic manifestations of BG are also nonspecific. However, there are two dominant patterns: nodular or masslike lesions (60% of cases) and pneumonic consolidations (27%) (61). Radiographic findings are usually unilateral (73% of cases) and seen in the upper lung zones (60%). The CT manifestations of BG consist of a focal mass or lobar consolidation with atelectasis

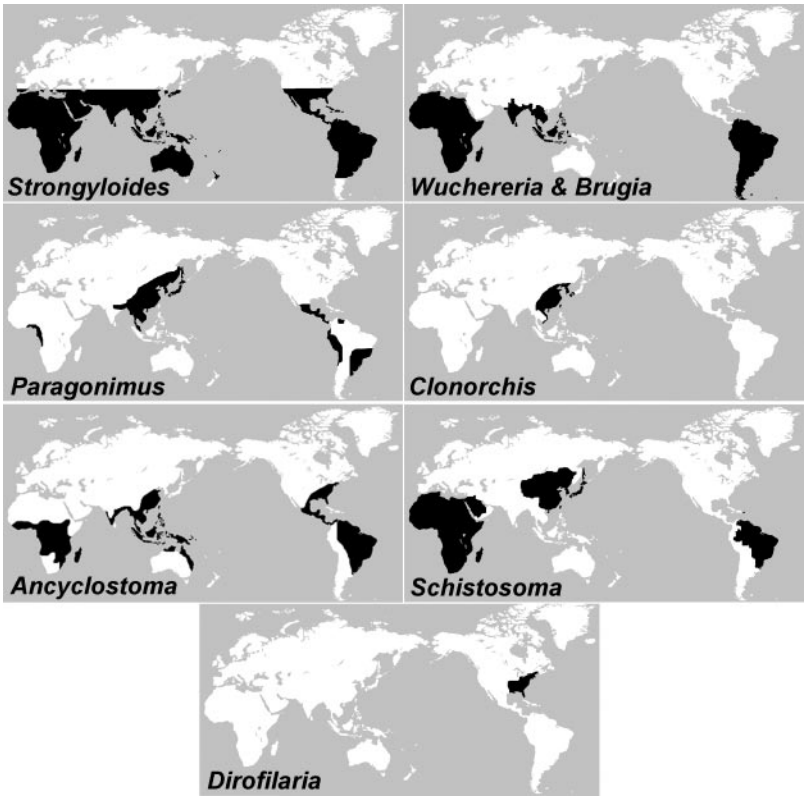


**Figure 12.** Maps illustrate the geographic distributions of common parasites. *Strongyloides* and *Wuchereria* infections are found in tropical and subtropical areas. The main endemic areas of paragonimiasis are East Asia, Southeast Asia, Latin America, and Africa. Clonorchiasis is endemic to Asia, including Korea, China, Taiwan, and Vietnam. *Ancylostoma* and *Schistosoma* infections are frequently seen in Africa, South America, and Asia. Dirofilariasis has been reported predominantly in the temperate climate of the East Coast and South in the United States. *Entamoeba* and *Toxocara* infections are distributed worldwide.

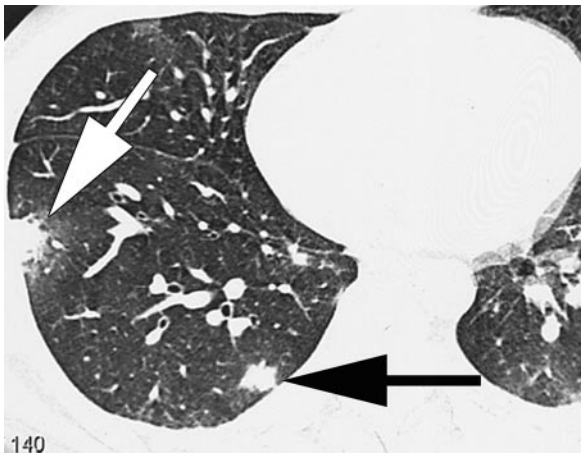


**Figure 13.** *C sinensis* infestation in a 25-year-old man. A skin test for *C sinensis* was strongly positive, and *Clonorchis*-specific IgG antibody by enzyme-linked immunosorbent assay was 0.27 (normal range, 0–0.25). Transverse thin-section (1-mm collimation) CT scan (lung windowing) shows multiple airspace nodules with surrounding ground-glass opacity in both lungs (arrows).

(Fig 11b) (62). However, the imaging features are nonspecific, and histologic confirmation is required.

## Parasitic Infections

Many parasites can cause pulmonary opacities with blood or tissue eosinophilia. Because the prevalence of individual parasitic infections varies from one geographic region to another, familiarity with the common parasites in one's geographic area of practice is critical to arriving at a correct diagnosis (Fig 12).

*Strongyloides stercoralis* infection can be accompanied by peripheral blood eosinophilia, rash, and transient pulmonary opacities (1). In patients with defects of cell-mediated immunity, *Strongyloides* hyperinfection syndrome can develop and is associated with diffuse pulmonary opacities, gram-negative sepsis, respiratory failure, and a high mortality rate (63).

In many developing countries, *Ascaris lumbricoides* is the most common cause of peripheral blood eosinophilia with pulmonary opacities. *A lumbricoides* was responsible for the pulmonary opacities in most of Loeffler's patients (1). Two mechanisms of pulmonary eosinophilic infiltration in parasitic infestations have been postulated: direct invasion (eg, *Ascaris, Schistosoma,* and *Filaria* species; *Paragonimus westermani; Ancylostoma duodenale*) and allergic reaction (*Entamoeba histolytica, Toxocara canis, Clonorchis sinensis*). In cases of *Clonorchis* infestation, immunologic stimulation from the life cycle of *C sinensis* in humans may cause the pulmonary opacities manifesting as single or multiple migrating nodules (Fig 13) (64).

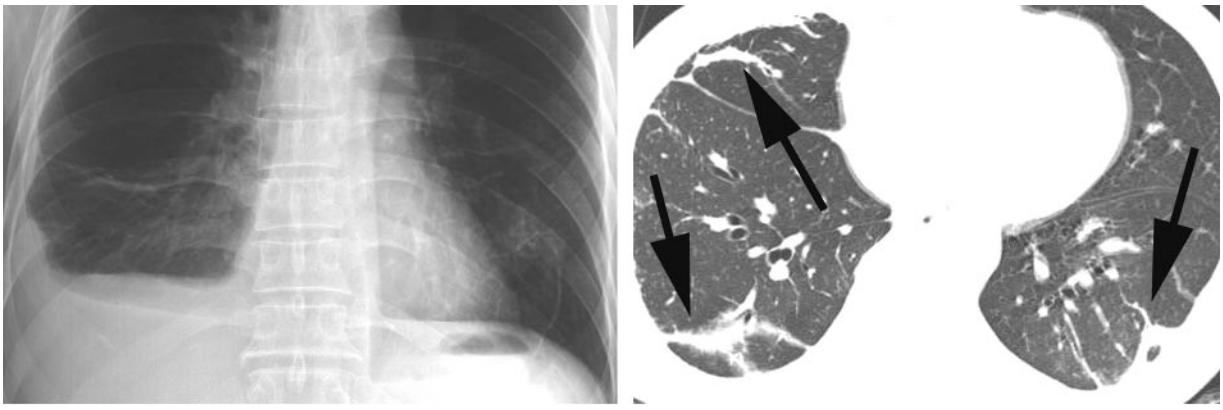

a. b.

**Figure 14.** PP in a 47-year-old man. **(a)** Chest radiograph shows several linear densities in both lungs as well as right-sided pleural effusion. **(b)** Transverse thin-section (1-mm collimation) CT scan (lung windowing) demonstrates subpleural linear opacities and tubular structures (arrows), both of which findings suggest worm migration tracts.

Tropical pulmonary eosinophilia is caused by the filarial worms *Wuchereria bancrofti* and *Brugia malayi*. Serum and BAL fluid contain high levels of IgE and IgG, which correlate with the disease activity (1). Peripheral blood eosinophil counts generally exceed 3000 cells per microliter, with an average BAL fluid eosinophilia of 50%. The earliest histologic finding in tropical pulmonary eosinophilia is an influx of histiocytes into the alveolar spaces. Large numbers of eosinophils subsequently invade the alveolar and interstitial spaces, frequently forming areas of eosinophilic abscesses. In long-standing disease, pulmonary fibrosis develops (65). Chest radiography shows fine, diffuse reticulonodular opacities in the lower lung zones (66).

Schistosomiasis is a helminthic infection that is endemic to tropical and subtropical regions. This infection can be divided into three categories: allergic dermatitis, acute schistosomiasis, and chronic schistosomiasis. Chronic and recurrent infection develops in persons living or traveling in endemic areas. In the lungs, granuloma formation and fibrosis around the *Schistosoma* eggs retained in the pulmonary vasculature may result in obliterative arteriolitis and pulmonary hypertension (67). Acute schistosomiasis is associated with primary exposure and is commonly seen in nonimmune travelers. The common CT findings in acute pulmonary schistosomiasis are small pulmonary nodules ranging from 2 to 15 mm and larger nodules with a ground-glass-opacity halo (68,69).

Pleuropulmonary paragonimiasis (PP) is a parasitic disease caused by *P westermani*. It is contracted through the ingestion of raw or partially cooked freshwater crabs or crayfish infected with

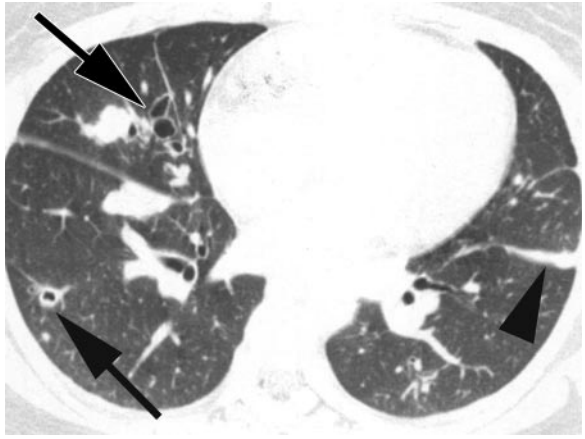

**Figure 15.** PP in a 42-year-old woman with 70% peripheral eosinophilia. A skin test for *P westermani* was positive. Transverse thin-section (1-mm collimation) CT scan (lung windowing) shows multiple nodules and thin-walled cysts (arrows) in the right middle and lower lobes. Note the linear opacity in the left lower lobe (arrowhead).

the metacercaria. Diagnosis is confirmed by the presence of parasitic eggs in the sputum, pleura, or BAL fluid. Intradermal and serologic tests are also available to help diagnose PP. The radiologic findings correlate well with the stage of the disease (70). Early findings are caused by the migration of juvenile worms and include pneumothorax or hydropneumothorax, focal airspace consolidation, and linear opacities (Fig 14). Later findings resulting from worm cysts include thin-walled cysts, masslike consolidation, nodules, and bronchiectasis (Fig 15). Typical CT findings in PP are a poorly marginated subpleural or subfissural

Teaching Point

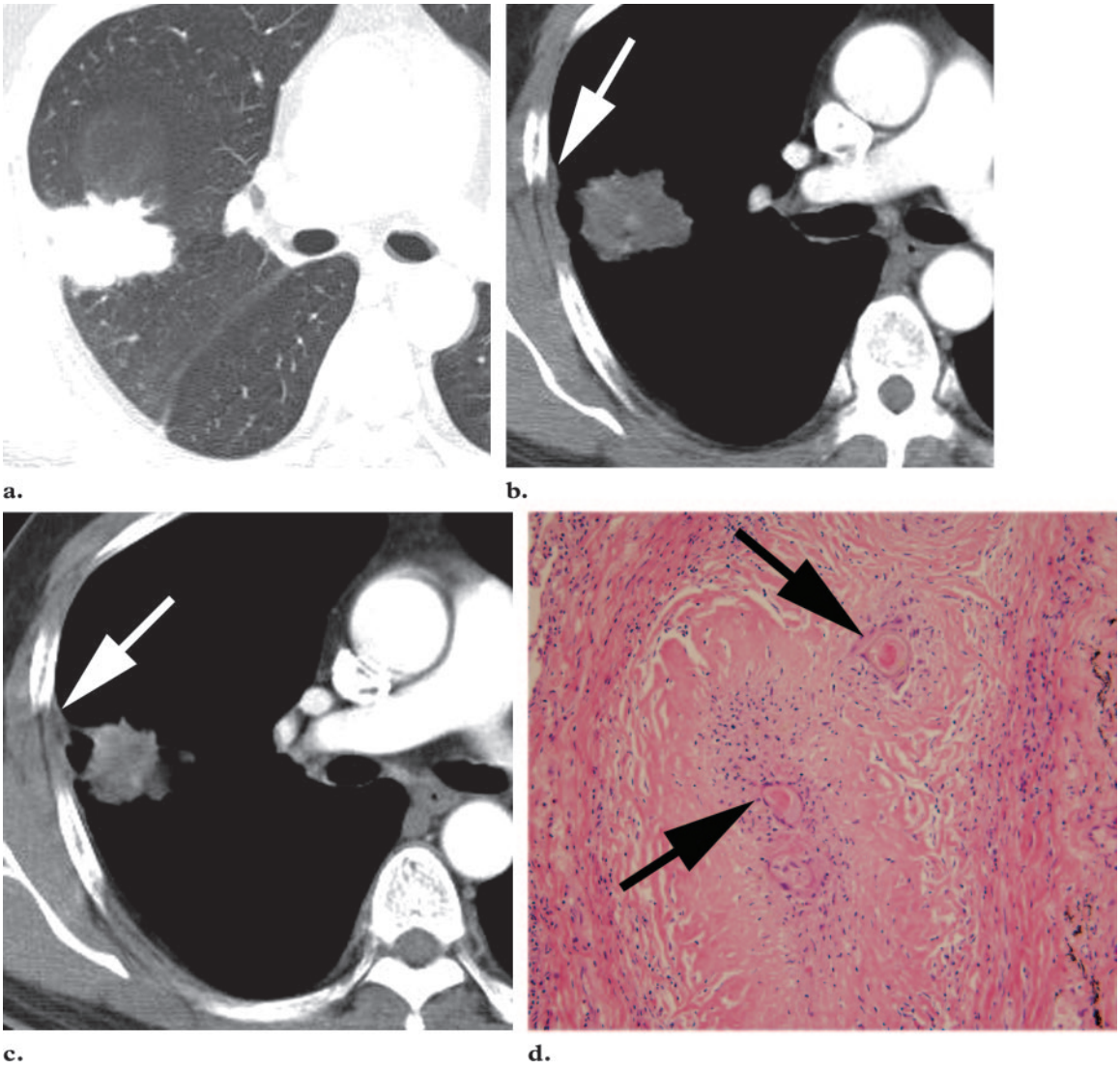


**Figure 16.** PP in a 46-year-old man with blood-tinged sputum and a history of ingestion of raw freshwater fish. **(a–c)** Chest CT scans (lung windowing in **a**, mediastinal windowing in **b** and **c**) show a low-opacity mass with a spiculated margin in the peripheral portion of the right upper lobe. Focal pleural thickening is also noted (arrow in **b** and **c**). **(d)** Photomicrograph (original magnification, ×200; H-E stain) of lung tissue obtained at open biopsy of the right upper lobe reveals eggs of *P westermani* (arrows) with associated necrotizing granulomatous inflammation and eosinophilic infiltrates.

nodule that frequently contains a low-opacity necrotic area, focal pleural thickening, and subpleural linear opacities leading to a necrotic peripheral pulmonary nodule (Fig 16) (71,72). In a study of the correlation between CT and histopathologic findings in PP, the subpleural nodule was a necrotic granuloma containing multiple eggs and organizing pneumonia with granulation tissue (Fig 16) (71). Adjacent pleural thickening was composed of fibrotic thickening with some areas of lymphocytic infiltration. Other common CT findings include adjacent bronchiectasis, areas of ground-glass opacity, and pleural effusion or pneumothorax. PP can mimic lung cancer by

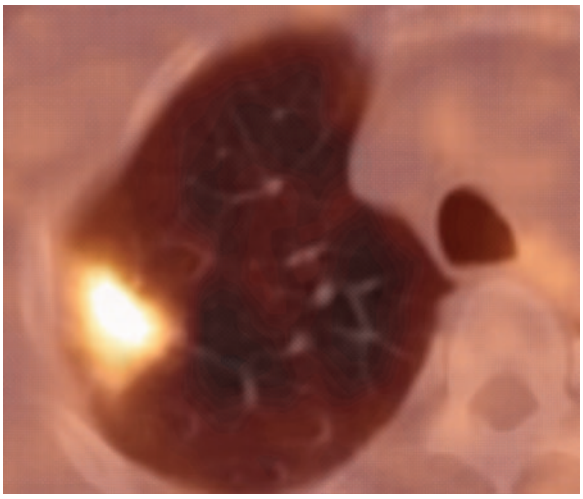

**Figure 17.** PP in a 44-year-old man. FDG PET scan demonstrates high glucose uptake (standardized uptake value = 5.6), a finding that suggests malignancy. Percutaneous aspiration biopsy revealed eosinophilic organizing pneumonia containing multiple eggs of *P westermani*.

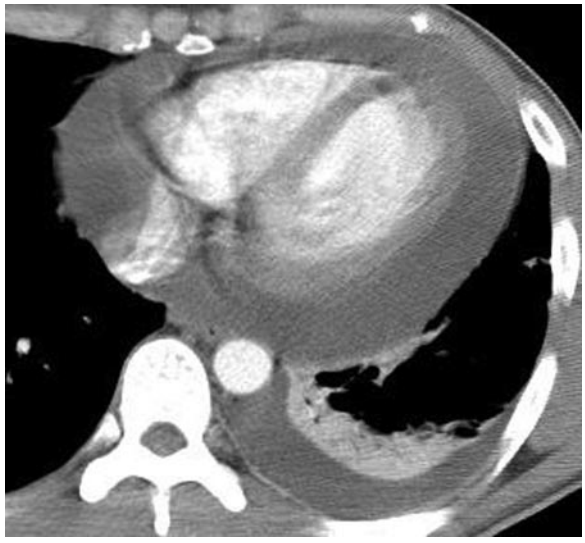

**Figure 18.** Pleural and pericardial paragonimiasis in a 31-year-old man with 20% peripheral eosinophilia. Contrast material–enhanced chest CT scan (mediastinal windowing) demonstrates pericardial and left pleural effusion with homogeneous thickening and enhancement of the pericardium and pleura. Eggs of *P westermani* were found in the pleural fluid.

showing high radiotracer uptake at 2-[fluorine-18]fluoro-2-deoxy-D-glucose (FDG) positron emission tomography (PET) (Fig 17) (71,73). Pleural and pericardial paragonimiasis without parenchymal lesions has also been reported (Fig 18) (74). The radiologic differential diagnosis includes bacterial infections with abscess formation, vasculitis, pulmonary tuberculosis, and cryptococcosis. However, a combination of typical CT findings and a history of eating freshwater crabs or wild boar meat in endemic areas may suggest the diagnosis of PP.

## Drug Reactions

A wide variety of drugs and toxic substances are important causes of pulmonary eosinophilic infiltrates. Patients with drug-induced eosinophilic lung disease can present with a variety of pathologic conditions ranging from a mild, SPE-like syndrome to a fulminant, AEP-like syndrome. There have been two significant outbreaks of drug-induced eosinophilic lung disease. The first outbreak was the toxic-oil syndrome associated with the oral ingestion of food-grade rapeseed oil contaminated with aniline derivatives (75). The second was the eosinophilia-myalgia syndrome associated with the ingestion of L-tryptophan (76). Cutaneous adverse drug reactions such as toxic epidermal necrolysis and DRESS (drug rash with eosinophilia and systemic symptoms) syndrome can be life threatening. Pulmonary involvement by cutaneous adverse drug reactions is rare (Fig 19) and is considered to be a severity factor (77). Many patients with drug-induced eosinophilic lung disease will improve by simply discontinuing the medication; in severe or persistent cases, however, short courses of corticosteroids appear to hasten recovery. The diagnosis is usually made on the basis of clinical history and blood eosinophilia rather than imaging findings.

At histologic analysis, drug-induced eosinophilic pneumonia is characterized by the accumulation of eosinophils and macrophages in the alveolar spaces (78). There is also usually an accompanying infiltrate composed of eosinophils, lymphocytes, and plasma cells within the alveolar septa and adjacent interstitium.

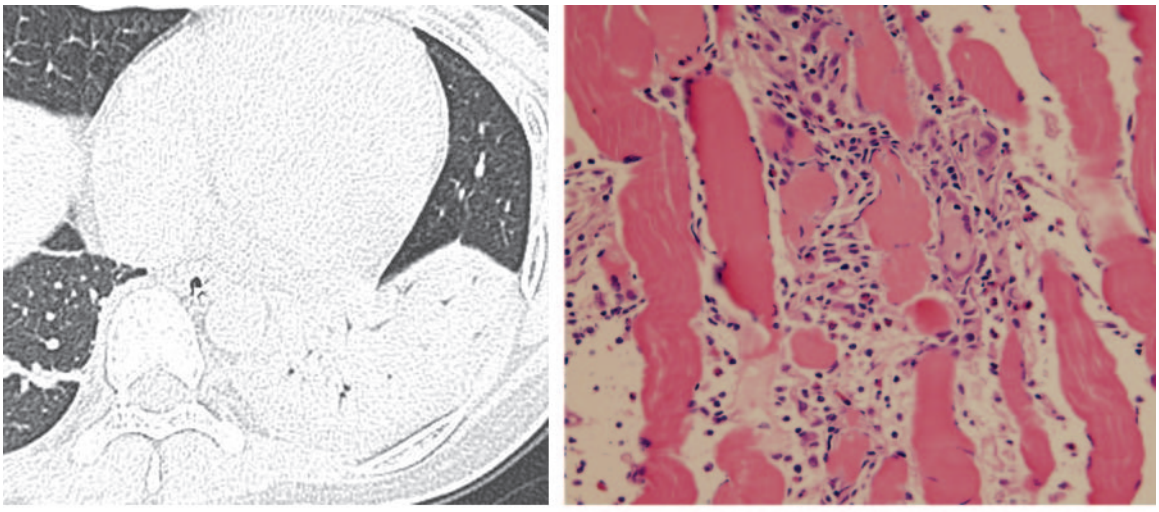

a. b.

**Figure 19.** DRESS syndrome caused by the antituberculous medication rifampin in a 30-year-old woman. The patient had 20% BAL fluid eosinophilia. **(a)** Transverse thin-section CT scan (lung windowing) shows consolidation with volume loss in the left lower lobe. **(b)** High-power photomicrograph (original magnification, ×400; H-E stain) of a muscle biopsy specimen reveals infiltrates composed of eosinophils, lymphocytes, and plasma cells within the muscle fiber. Similar findings were seen in the periportal area, alveolar septa and adjacent interstitium, and dermis at microscopic analysis of biopsy specimens obtained from the liver, lung, and skin, respectively.

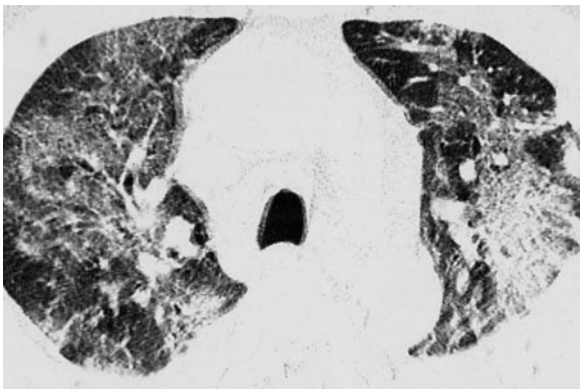

**Figure 20.** Ampicillin-induced pneumonia in a 69-year-old man with 24.1% peripheral eosinophilia. Transverse thin-section (1-mm collimation) CT scan (lung windowing) demonstrates multifocal patchy areas of ground-glass opacity with thickening of the interlobular and intralobular interstitium.

Chest radiography demonstrates variable and nonspecific findings that include consolidation, hilar adenopathy, pleural effusion, and reticulonodular densities. CT more clearly reveals the pattern and extent of the variable findings, including areas of ground-glass opacity, consolidation, nodules, and irregular lines (Fig 20) (13). In one series, airspace consolidation and ground-glass opacity in a predominantly peripheral distribution were the most common high-resolution CT findings (79).

## Eosinophilic Vasculitis

Churg-Strauss syndrome was first described in 1951 by Churg and Strauss on the basis of the histologic criteria of tissue infiltration by eosinophils, necrotizing vasculitis, and extravascular granulomas (80). The diagnosis of Churg-Strauss syndrome can be made if four or more of the following six findings are present: asthma, eosinophilia greater than 10% of the white blood cell differential count, neuropathy, migratory or transient pulmonary opacities, paranasal sinus abnormalities, and extravascular eosinophils revealed at biopsy (81). The etiology of Churg-Strauss

**Table 2**
**Thoracic and Extrathoracic Manifestations of Churg-Strauss Syndrome**

| Anatomic Location | Manifestations |
|---|---|
| Lung | Pulmonary vasculitis, pleural effusion, hilar lymphadenopathy |
| Heart | Acute pericarditis, constrictive pericarditis, cardiac failure, myocardial infarction |
| Central nervous system | Mononeuritis complex |
| Gastrointestinal tract | Eosinophilic gastroenteritis, polyarteritis nodosa |
| Skin | Purpura, macular or papular erythematous rash, urticaria, subcutaneous nodules |
| Kidney | Focal segmental glomerulonephritis |
| Muscles and joints | Myalgia, joint pain |

syndrome is still unknown, but an allergic or immune pathogenesis for the disease has been suggested by the presence of asthma, eosinophilia, and elevated serum IgE levels in some cases (82). Several recent reports have suggested an association between the use of leukotriene receptor antagonists for treating asthma and Churg-Strauss syndrome (83–85). Asthma is the central feature of Churg-Strauss syndrome. The relatively late patient age at onset distinguishes the asthma in patients with Churg-Strauss syndrome from that in the general population. Whereas asthma is often accompanied by eosinophilia that seldom exceeds $0.8 \times 10^9$ cells per liter, the eosinophilia in Churg-Strauss syndrome is generally of a much higher order (37).

The lung is the most commonly involved organ, followed by the skin. However, any organ can be involved, including the central nervous system, heart, and gastrointestinal tract (Table 2). CEP is commonly associated with asthma and tissue eosinophilia but does not manifest with granulomatous arteritis and is not associated with extrapulmonary lesions.

At radiography, Churg-Strauss syndrome usually appears as bilateral nonsegmental consolidation or reticulonodular opacities (37). The most common thin-section CT findings include subpleural ground-glass opacity or consolidation with a lobular distribution, centrilobular nodules, bronchial wall thickening, and interlobular septal thickening (Figs 21, 22). Less common findings include hyperinflation, mediastinal or hilar lymphadenopathy, and pleural or pericardial effusion (37,86). The radiologic differential diagnosis includes CEP and other types of pulmonary angiitis and granulomatosis (37). At CT, CEP is characterized by the presence of homogeneous peripheral airspace consolidation, whereas in Churg-Strauss syndrome, peripheral consolidation has a tendency toward lobular distribution and the frequent presence of centrilobular nodules within the ground-glass opacity. Solitary or multiple nodules with frequent cavitation are the most common finding in Wegener granulomatosis, lymphomatoid granulomatosis, and necrotizing sarcoid granulomatosis; in Churg-Strauss syndrome, on the other hand, the most common finding is peripheral consolidation, with multiple nodules occurring rather infrequently (37).

**Teaching Point**

## Conclusions

Patients may first be recognized as having an eosinophilic lung disease on the basis of pulmonary symptoms or chest radiographic abnormalities accompanied by an increased number of blood,

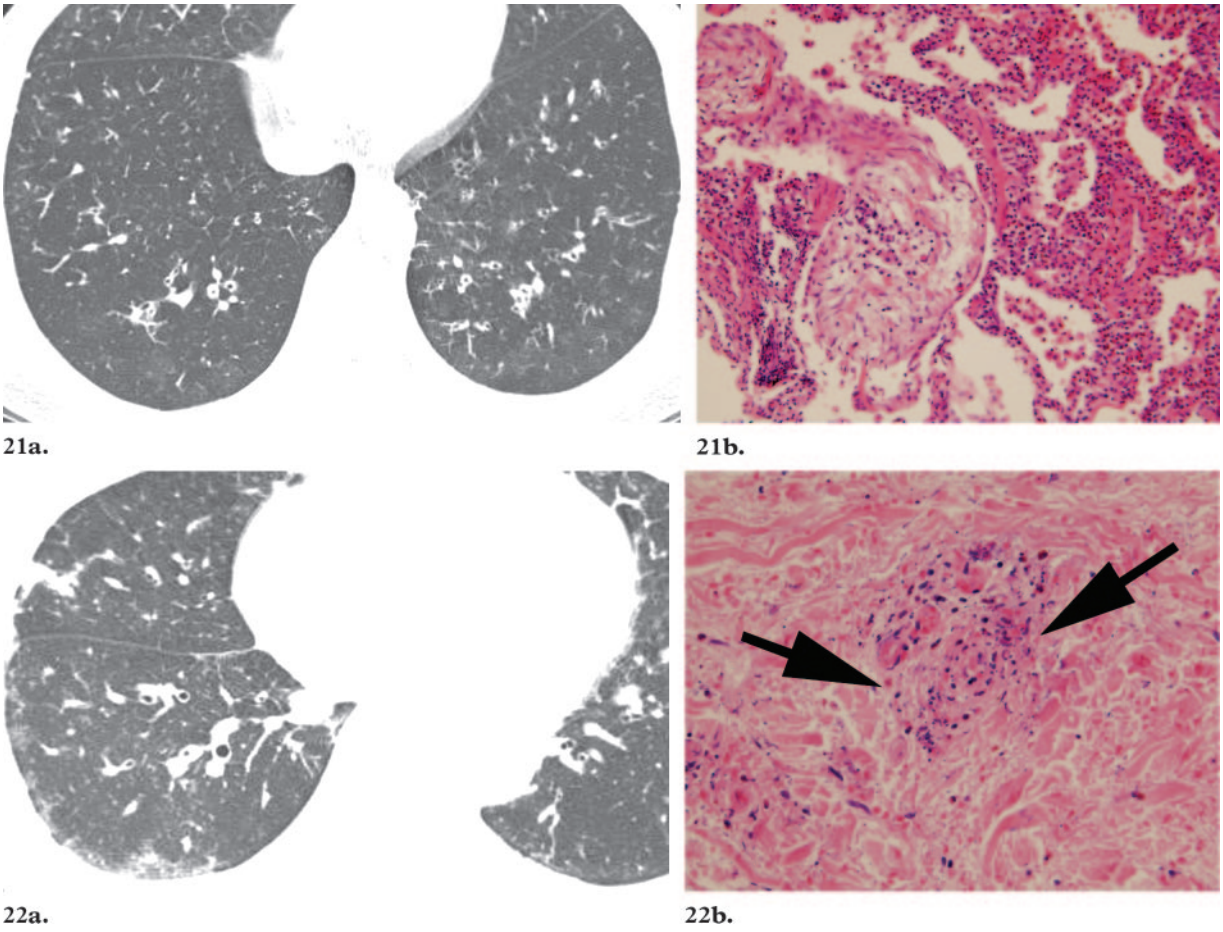

21a. 21b.

22a. 22b.

**Figures 21, 22.** **(21)** Churg-Strauss syndrome in a 30-year-old asthmatic man who presented with chronic cough, dyspnea, and skin rash. The patient had 17% peripheral and 32% BAL fluid eosinophilia. **(a)** Thin-section (1-mm collimation) CT scan (lung windowing) demonstrates multiple small centrilobular nodules, bronchial wall thickening, and ground-glass opacity in both lung bases. **(b)** Photomicrograph (original magnification, ×200; H-E stain) of an open biopsy specimen obtained from the right lower lobe 3 months after **a** shows eosinophilic organizing pneumonia. **(22)** Churg-Strauss syndrome in a 49-year-old asthmatic woman with quadriparesis and skin rash. The patient had a leukocyte count of 15,640 leukocytes per microliter and 49% peripheral eosinophilia. **(a)** Thin-section CT scan (lung windowing) shows subpleural ground-glass opacity, focal lobular consolidation, centrilobular nodules, and bronchial wall thickening in both lung bases. **(b)** High-power photomicrograph (original magnification, ×400; H-E stain) of a biopsy specimen obtained from the skin of the leg reveals necrotizing vasculitis (arrows) involving small dermal vessels. Peripheral nerve biopsy revealed eosinophilic vasculitis.

BAL fluid, or tissue eosinophils. Although several radiologic findings can help identify idiopathic eosinophilic lung disease, there is considerable overlap of these findings in the various entities, which precludes a confident diagnosis in the majority of cases. Correlation between CT findings and the results of careful clinical evaluation may be helpful in developing a differential diagnosis for eosinophilic lung disease, although there are diagnostic pitfalls in the form of some overlapping features (Table 3).

**Table 3**
**Overview of Eosinophilic Lung Diseases**

| Clinical Entity | Clinical, Pathologic, and Radiologic Features | | | | | | |
|---|---|---|---|---|---|---|---|
| | Asthma | Initial Peripheral Eosinophilia | BAL Fluid Eosinophilia | Increased IgE Level | Extrathoracic Manifestations | Pathologic Findings | CT Findings |
| SPE | No | Yes | >20% | Yes | No | Infiltration of eosinophils into the alveolar septa and interstitium | Nodules with a GGO halo, transient and migratory |
| AEP | No | No | >25% | Some | No | Diffuse alveolar damage with interstitial and alveolar eosinophils | Bilateral patchy areas of GGO, interlobular septal thickening |
| CEP | Yes (50%) | Yes | >25% | Yes (approximately 67%) | No | Infiltration of eosinophils into the alveoli and interstitium with interstitial fibrosis | Homogeneous peripheral airspace consolidation |
| IHS | No | Yes | High (up to 73%) | Yes (50%) | Yes | Eosinophilic infiltration with disruption of architecture | Nodules with a GGO halo |
| ABPA | Yes (100%) | Yes | <20% | Yes | No | Bronchocentric granuloma with eosinophils, fungal hyphae | Bronchiectasis with or without mucoid impaction involving the central and upper lungs |
| BG | Yes (approximately 33%) | Yes | <20% | Some | No | Granulomatous inflammation of bronchial and bronchiolar epithelium | Nonspecific: focal mass or lobular consolidation with atelectasis |
| Parasitic infections | No | Yes | <20% | Yes | No | Variable depending on type of parasitic infestation | Variable depending on type of parasitic infestation |
| Drug reactions | No | Yes | <20% | Yes | No | Infiltration of eosinophils and macrophages into the alveoli | Nonspecific: peripheral airspace consolidation and GGO |
| CSS | Yes (100%) | Yes | >30% | Yes | Yes | Necrotizing vasculitis, extravascular granulomas, eosinophilic pneumonia | Subpleural consolidation with a lobular distribution, centrilobular nodules |

Note.—CSS = Churg-Strauss syndrome, GGO = ground-glass opacity.

## References


1. Allen JN, Davis WB. Eosinophilic lung diseases. Am J Respir Crit Care Med 1994;150:1423–1438.
2. Allen JN, Davis WB, Pacht ER. Diagnostic significance of increased bronchoalveolar lavage fluid eosinophils. Am Rev Respir Dis 1990;142:642–647.
3. Davis WB, Fells GA, Sun XH, Gadek JE, Venet A, Crystal RG. Eosinophil-mediated injury to lung parenchymal cells and interstitial matrix: a possible role for eosinophils in chronic inflammatory disorders of the lower respiratory tract. J Clin Invest 1984;74:269–278.
4. Friedman PJ, Liebow AA, Sokoloff J. Eosinophil granuloma of lung: clinical aspects of primary histiocytosis in the adult. Medicine 1981;60:385–396.
5. Lombard CM, Tazelaar HD, Krasne DL. Pulmonary eosinophilia in coccidioidal infections. Chest 1987;91:734–736.
6. Fleury-Feith J, Van Nhieu JT, Picard C, Escudier E, Bernaudin JF. Bronchoalveolar lavage eosinophilia associated with Pneumocystis carinii pneumonitis in AIDS patients: comparative study with non-AIDS patients. Chest 1989;95:1198–1201.
7. Weller PF. The immunobiology of eosinophils. N Engl J Med 1991;324:1110–1118.
8. Takayanagi N, Kanazawa M, Kawabata Y, Colby TV. Chronic bronchiolitis with associated eosinophilic lung disease (eosinophilic bronchiolitis). Respiration 2001;68:319–322.
9. Johkoh T, Muller NL, Akira M, et al. Eosinophilic lung diseases: diagnostic accuracy of thin-section CT in 111 patients. Radiology 2000;216:773–780.
10. Ford RM. Transient pulmonary eosinophilia and asthma: a review of 20 cases occurring in 5,702 asthma sufferers. Am Rev Respir Dis 1966;93:797–803.
11. Cordier JF. Eosinophilic pneumonias. In: Schwarz M, King T, eds. Interstitial lung disease. 4th ed. Toronto, Canada: Decker, 2003; 657–700.
12. Bain GA, Flower CD. Pulmonary eosinophilia. Eur J Radiol 1996;23:3–8.
13. Kim Y, Lee KS, Choi DC, Primack SL, Im JG. The spectrum of eosinophilic lung disease: radiologic findings. J Comput Assist Tomogr 1997;21:920–930.
14. Kim Y, Lee KS, Jung KJ, Han J, Kim JS, Suh JS. Halo sign on high resolution CT: findings in spectrum of pulmonary diseases with pathologic correlation. J Comput Assist Tomogr 1999;23(4):622–626.
15. Allen JN, Pacht ER, Gadek JE, Davis WB. Acute eosinophilic pneumonia as a reversible cause of noninfectious respiratory failure. N Engl J Med 1989;321:569–574.
16. Ogawa H, Fujimura M, Matsuda T, Nakamura H, Kumabashiri I, Kitagawa S. Transient wheeze: eosinophilic bronchobronchiolitis in acute eosinophilic pneumonia. Chest 1993;104:493–496.
17. Philit F, Etienne-Mastroianni B, Parrot A, Guerin C, Robert D, Cordier JF. Idiopathic acute eosinophilic pneumonia: a study of 22 patients. Am J Respir Crit Care Med 2002;166(9):1235–1239.
18. Nakajima M, Manabe T, Niki Y, Matsushima T. Cigarette smoke–induced acute eosinophilic pneumonia. Radiology 1998;207:829–831.
19. Shintani H, Fujimura M, Yasui M, et al. Acute eosinophilic pneumonia caused by cigarette smoking. Intern Med 2000;39:66–68.
20. Rom WN, Weiden M, Garcia R, et al. Acute eosinophilic pneumonia in a New York City firefighter exposed to World Trade Center dust. Am J Respir Crit Care Med 2002;166(6):797–800.
21. Hirai K, Yamazaki Y, Okada K, Furuta S, Kubo K. Acute eosinophilic pneumonia associated with smoke from fireworks. Intern Med 2000;39:401–403.
22. Tazelaar HD, Linz LJ, Colby TV, Myers JL, Limper AH. Acute eosinophilic pneumonia: histopathologic findings in nine patients. Am J Respir Crit Care Med 1997;155:296–302.
23. Cheon JE, Lee KS, Jung GS, Chung MH, Cho YD. Acute eosinophilic pneumonia: radiographic and CT findings in six patients. AJR Am J Roentgenol 1996;167:1195–1199.
24. King MA, Pope-Harman AL, Allen JN, Christoforidis GA, Christoforidis AJ. Acute eosinophilic pneumonia: radiologic and clinical features. Radiology 1997;203:715–719.
25. Carrington CB, Addington WW, Goff AM, et al. Chronic eosinophilic pneumonia. N Engl J Med 1969;280:787–798.
26. Jederlinic PJ, Sicilian L, Gaensler EA. Chronic eosinophilic pneumonia: a report of 19 cases and a review of the literature. Medicine 1988;67:154–162.
27. Fox B, Seed WA. Chronic eosinophilic pneumonia. Thorax 1980;35:570–580.
28. Naughton M, Fahy J, FitzGerald MX. Chronic eosinophilic pneumonia: a long-term follow-up of 12 patients. Chest 1993;103:162–165.
29. Brezis M, Lafair J. Thrombocytosis in chronic eosinophilic pneumonia. Chest 1979;76:231–232.
30. Dejaegher P, Demedts M. Bronchoalveolar lavage in eosinophilic pneumonia before and during corticosteroid therapy. Am Rev Respir Dis 1984;129:631–632.
31. Mochimaru H, Kawamoto M, Fukuda Y, Kudoh S. Clinicopathological differences between acute and chronic eosinophilic pneumonia. Respirology 2005;10:76–85.
32. Gaensler EA, Carrington CB. Peripheral opacities in chronic eosinophilic pneumonia: the photographic negative of pulmonary edema. AJR Am J Roentgenol 1977;128:1–13.
33. Ebara H, Ikezoe J, Johkoh T, et al. Chronic eosinophilic pneumonia: evolution of chest radiograms and CT features. J Comput Assist Tomogr 1994;18:737–744.
34. McCarthy DS, Pepys J. Cryptogenic pulmonary eosinophilias. Clin Allergy 1973;3:339–351.
35. Mayo JR, Muller NL, Road J, Sisler J, Lillington G. Chronic eosinophilic pneumonia: CT findings in six cases. AJR Am J Roentgenol 1989;153:727–730.
36. Samman YS, Wali SO, Abdelaal MA, Gangi MT, Krayem AB. Chronic eosinophilic pneumonia presenting with recurrent massive bilateral pleural effusion. Chest 2001;119:968–970.
37. Choi YH, Im JG, Han BK, Kim JH, Lee KY, Myoung NH. Thoracic manifestation of Churg-Strauss syndrome: radiologic and clinical findings. Chest 2000;117:117–124.
38. Winn RE, Kollef MH, Meyer JI. Pulmonary involvement in the hypereosinophilic syndrome. Chest 1994;105:656–660.

39. Chusid MJ, Dale DC, West BC, Wolff SM. The hypereosinophilic syndrome: analysis of fourteen cases with review of the literature. Medicine 1975; 54:1–27.
40. Spry CJ, Davies J, Tai PC, Olsen EG, Oakley CM, Goodwin JF. Clinical features of fifteen patients with the hypereosinophilic syndrome. Q J Med 1983 Winter;52(205):1–22.
41. Parrillo JE, Borer JS, Henry WL, Wolff SM, Fauci AS. The cardiovascular manifestations of the hypereosinophilic syndrome: prospective study of 26 patients, with review of the literature. Am J Med 1979;67:572–582.
42. Fauci AS, Harley JB, Roberts WC, Ferrans VJ, Gralnick HR, Bjornson BH. The idiopathic hypereosinophilic syndrome: clinical, pathophysiologic, and therapeutic considerations. Ann Intern Med 1982;97:78–92.
43. Spry CJ. The hypereosinophilic syndrome: clinical features, laboratory findings and treatment. Allergy 1982;37:539–551.
44. Slabbynck H, Impens N, Naegels S, Dewaele M, Schandevyl W. Idiopathic hypereosinophilic syndrome-related pulmonary involvement diagnosed by bronchoalveolar lavage. Chest 1992;101:1178–1180.
45. Epstein DM, Taormina V, Gefter WB, Miller WT. The hypereosinophilic syndrome. Radiology 1981;140:59–62.
46. Kang EY, Shim JJ, Kim JS, Kim KI. Pulmonary involvement of idiopathic hypereosinophilic syndrome: CT findings in five patients. J Comput Assist Tomogr 1997;21(4):612–615.
47. Wang JL, Patterson R, Rosenberg M, Roberts M, Cooper BJ. Serum IgE and IgG antibody activity against Aspergillus fumigatus as a diagnostic aid in allergic bronchopulmonary aspergillosis. Am Rev Respir Dis 1978;117:917–927.
48. Rosenberg M, Patterson R, Mintzer R, Cooper BJ, Roberts M, Harris KE. Clinical and immunologic criteria for the diagnosis of allergic bronchopulmonary aspergillosis. Ann Intern Med 1977;86:405–414.
49. Ricketti AJ, Greenberger PA, Patterson R. Serum IgE as an important aid in management of allergic bronchopulmonary aspergillosis. J Allergy Clin Immunol 1984;74:68–71.
50. Bosken CH, Myers JL, Greenberger PA, Katzenstein AL. Pathologic features of allergic bronchopulmonary aspergillosis. Am J Surg Pathol 1988; 12:216–222.
51. Patterson R, Greenberger PA, Radin RC, Roberts M. Allergic bronchopulmonary aspergillosis: staging as an aid to management. Ann Intern Med 1982;96:286–291.
52. McCarthy DS, Simon G, Hargreave FE. The radiological appearances in allergic bronchopulmonary aspergillosis. Clin Radiol 1970;21:366–375.
53. Mendelson EB, Fisher MR, Mintzer RA, Halwig JM, Greenberger PA. Roentgenographic and clinical staging of allergic bronchopulmonary aspergillosis. Chest 1985;87:334–339.
54. Neeld DA, Goodman LR, Gurney JW, Greenberger PA, Fink JN. Computerized tomography in the evaluation of allergic bronchopulmonary aspergillosis. Am Rev Respir Dis 1990;142:1200–1205.
55. Mintzer RA, Rogers LF, Kruglik GD, Rosenberg M, Neiman HL, Patterson R. The spectrum of radiologic findings in allergic bronchopulmonary aspergillosis. Radiology 1978;127:301–307.
56. Franquet T, Muller NL, Gimenez A, Guembe P, de La Torre J, Bague S. Spectrum of pulmonary aspergillosis: histologic, clinical, and radiologic findings. RadioGraphics 2001;21:825–837.
57. Angus RM, Davies ML, Cowan MD, McSharry C, Thomson NC. Computed tomographic scanning of the lung in patients with allergic bronchopulmonary aspergillosis and in asthmatic patients with a positive skin test to Aspergillus fumigatus. Thorax 1994;49:586–589.
58. Ward S, Heyneman L, Lee MJ, Leung AN, Hansell DM, Muller NL. Accuracy of CT in the diagnosis of allergic bronchopulmonary aspergillosis in asthmatic patients. AJR Am J Roentgenol 1999; 173:937–942.
59. Liebow AA. The J. Burns Amberson lecture: pulmonary angiitis and granulomatosis. Am Rev Respir Dis 1973;108:1–18.
60. Katzenstein AL, Liebow AA, Friedman PJ. Bronchocentric granulomatosis, mucoid impaction and hypersensitivity reaction to fungi. Am Rev Respir Dis 1975;111:497–537.
61. Robinson RG, Wehunt WD, Tsou E, Koss MN, Hochholzer L. Bronchocentric granulomatosis: roentgenographic manifestations. Am Rev Respir Dis 1982;125:751–756.
62. Ward S, Heyneman LE, Flint JD, Leung AN, Kazerooni EA, Muller NL. Bronchocentric granulomatosis: computed tomographic findings in five patients. Clin Radiol 2000;55:296–300.
63. Jamil SA, Hilton E. The strongyloides hyperinfection syndrome. N Y State J Med 1992;92:67–68.
64. Lee HK, Jin SL, Lee HP, Choi SJ, Yum HK. Loffler's syndrome associated with Clonorchis sinensis infestation. Korean J Intern Med 2003;18:255–259.
65. Udwadia FE. Tropical eosinophilia: a correlation of clinical, histopathologic and lung function studies. Dis Chest 1967;52:531–538.
66. Khoo FY, Danaraj TJ. The roentgenographic appearance of eosinophilic lung (tropical eosinophilia). Am J Roentgenol Radium Ther Nucl Med 1960;83:251–259.
67. Gopinath R, Nutman TB. Parasitic diseases. In: Murray JF, Nadel JA, eds. Textbook of respiratory medicine. 3rd ed. Philadelphia, Pa: Saunders, 2000; 1143–1171.
68. Nguyen LQ, Estrella J, Jett EA, Grunvald EL, Nicholson L, Levin DL. Acute schistosomiasis in nonimmune travelers: chest CT findings in 10 patients. AJR Am J Roentgenol 2006;186:1300–1303.
69. Waldman AD, Day JH, Shaw P, Bryceson AD. Subacute pulmonary granulomatous schistosomiasis: high resolution CT appearances—another cause of the halo sign. Br J Radiol 2001;74:1052–1055.
70. Im JG, Kong Y, Shin YM, et al. Pulmonary paragonimiasis: clinical and experimental studies. RadioGraphics 1993;13:575–586.
71. Kim TS, Han J, Shim SS, et al. Pleuropulmonary paragonimiasis: CT findings in 31 patients. AJR Am J Roentgenol 2005;185:616–621.

72. Im JG, Whang HY, Kim WS, Han MC, Shim YS, Cho SY. Pleuropulmonary paragonimiasis: radiologic findings in 71 patients. AJR Am J Roentgenol 1992;159:39–43.
73. Watanabe S, Nakamura Y, Kariatsumari K, et al. Pulmonary paragonimiasis mimicking lung cancer on FDG-PET imaging. Anticancer Res 2003;23:3437–3440.
74. Iwahashi N, Suzuki F, Tamura S, et al. A case of paragonimiasis Miyazakii with bilateral pleural and pericardial effusion [in Japanese]. Nihon Kyobu Shikkan Gakkai Zasshi 1991;29:1047–1051.
75. Kilbourne EM, Rigau-Perez JG, Heath CW Jr, et al. Clinical epidemiology of toxic-oil syndrome: manifestations of a new illness. N Engl J Med 1983;309:1408–1414.
76. Silver RM, Heyes MP, Maize JC, Quearry B, Vionnet-Fuasset M, Sternberg EM. Scleroderma, fasciitis, and eosinophilia associated with the ingestion of tryptophan. N Engl J Med 1990;322:874–881.
77. Wolkenstein P, Chosidow O. Cutaneous adverse drug reaction with pulmonary involvement [in French]. Rev Mal Respir 2003;20(5 pt 1):719–726.
78. Pietra GG. Pathologic mechanisms of drug-induced lung disorders. J Thorac Imaging 1991;6:1–7.
79. Souza CA, Muller NL, Johkoh T, Akira M. Drug-induced eosinophilic pneumonia: high-resolution CT findings in 14 patients. AJR Am J Roentgenol 2006;186:368–373.
80. Churg J, Strauss L. Allergic granulomatosis, allergic angiitis, and periarteritis nodosa. Am J Pathol 1951;27:277–301.
81. Masi AT, Hunder GG, Lie JT, et al. The American College of Rheumatology 1990 criteria for the classification of Churg-Strauss syndrome (allergic granulomatosis angiitis). Arthritis Rheum 1990;33:1094–1100.
82. Chumbley LC, Harrison EG Jr, DeRemee RA. Allergic granulomatosis and angiitis (Churg-Strauss syndrome): report and analysis of 30 cases. Mayo Clin Proc 1977;52:477–484.
83. Shimbo J, Onodera O, Tanaka K, Tsuji S. Churg-Strauss syndrome and the leukotriene receptor antagonist pranlukast. Clin Rheumatol 2005;24:661–662.
84. Kinoshita M, Shiraishi T, Koga T, Ayabe M, Rikimaru T, Oizumi K. Churg-Strauss syndrome after corticosteroid withdrawal in an asthmatic patient treated with pranlukast. J Allergy Clin Immunol 1999;103:534–535.
85. Wechsler ME, Garpestad E, Flier SR, et al. Pulmonary infiltrates, eosinophilia, and cardiomyopathy following corticosteroid withdrawal in patients with asthma receiving zafirlukast. JAMA 1998;279:455–457.
86. Worthy SA, Muller NL, Hansell DM, Flower CD. Churg-Strauss syndrome: the spectrum of pulmonary CT findings in 17 patients. AJR Am J Roentgenol 1998;170:297–300.

*This article meets the criteria for 1.0 credit hour in category 1 of the AMA Physician's Recognition Award. To obtain credit, see accompanying test at http://www.rsna.org/education/rg_cme.html.*

RadioGraphics

# Eosinophilic Lung Diseases: A Clinical, Radiologic, and Pathologic Overview

*Yeon Joo Jeong, MD et al*

**RadioGraphics 2007;** 27:617–639 • **Published online** 10.1148/rg.273065051 • **Content Codes:** CH CT

**Page 618**
The diagnosis of eosinophilic lung disease can be made if any of the following findings is present: (a) pulmonary opacities with peripheral eosinophilia, (b) tissue eosinophilia confirmed at either open or transbronchial lung biopsy, or (c) increased eosinophils in bronchoalveolar lavage (BAL) fluid (1).

**Page 618**
Eosinophilic lung diseases are generally classified as those of unknown cause (simple pulmonary eosinophilia [SPE], acute eosinophilic pneumonia [AEP], chronic eosinophilic pneumonia [CEP], idiopathic hypereosinophilic syndrome [IHS]) and those of known cause (allergic bronchopulmonary aspergillosis [ABPA], bronchocentric granulomatosis [BG], parasitic infection, drug reaction), as well as eosinophilic vasculitis (allergic angiitis, granulomatosis) (Table 1).

**Page 622**
At CT, CEP is characterized by the presence of homogeneous peripheral airspace consolidation, whereas in Churg-Strauss syndrome, peripheral consolidation has a tendency toward lobular distribution and, frequently, associated centrilobular nodules within the ground-glass opacity (37). The distribution of opacities is identical to that in Loeffler syndrome, although in the latter, the pulmonary opacities are transient and shift over days, whereas untreated CEP has a more protracted course (35).

**Page 628**
The radiologic findings correlate well with the stage of the disease (70). Early findings are caused by the migration of juvenile worms and include pneumothorax or hydropneumothorax, focal airspace consolidation, and linear opacities (Fig 14). Later findings resulting from worm cysts include thin-walled cysts, masslike consolidation, nodules, and bronchiectasis (Fig 15).

**Page 632**
The radiologic differential diagnosis includes CEP and other types of pulmonary angiitis and granulomatosis (37). At CT, CEP is characterized by the presence of homogeneous peripheral airspace consolidation, whereas in Churg-Strauss syndrome, peripheral consolidation has a tendency toward lobular distribution and the frequent presence of centrilobular nodules within the ground-glass opacity. Solitary or multiple nodules with frequent cavitation are the most common finding in Wegener granulomatosis, lymphomatoid granulomatosis, and necrotizing sarcoid granulomatosis; in Churg-Strauss syndrome, on the other hand, the most common finding is peripheral consolidation, with multiple nodules occurring rather infrequently (37).

# RadioGraphics 2007

## This is your reprint order form or pro forma invoice

**(Please keep a copy of this document for your records.)**

Reprint order forms and purchase orders or prepayments must be received 72 hours after receipt of form either by mail or by fax at 410-820-9765. It is the policy of Cadmus Reprints to issue one invoice per order. **Please print clearly**.

Author Name _____
Title of Article _____
Issue of Journal_____ Reprint # _____ Publication Date _____
Number of Pages_____ KB # _____ Symbol RadioGraphics
Color in Article? Yes / No (Please Circle)

**Please include the journal name and reprint number or manuscript number on your purchase order or other correspondence.**

## Order and Shipping Information

### Reprint Costs (Please see page 2 of 2 for reprint costs/fees.)

_____ Number of reprints ordered $_____
_____ Number of color reprints ordered $_____
_____ Number of covers ordered $_____
**Subtotal** $_____
Taxes $_____

(*Add appropriate sales tax for Virginia, Maryland, Pennsylvania, and the District of Columbia or Canadian GST to the reprints if your order is to be shipped to these locations*.)

First address included, add $32 for each additional shipping address $_____

**TOTAL** $_____

### Shipping Address (cannot ship to a P.O. Box) Please Print Clearly

Name _____
Institution _____
Street _____
City _____ State _____ Zip _____
Country _____
Quantity_____ Fax _____
Phone: Day _____ Evening _____
E-mail Address _____

### Additional Shipping Address* (cannot ship to a P.O. Box)

Name _____
Institution _____
Street _____
City _____ State _____ Zip _____
Country _____
Quantity _____ Fax _____
Phone: Day _____ Evening _____
E-mail Address _____

** Add $32 for each additional shipping address*

## Payment and Credit Card Details

**Enclosed**: Personal Check _____
Credit Card Payment Details _____
Checks must be paid in U.S. dollars and drawn on a U.S. Bank.

Credit Card: __ VISA __ Am. Exp. __ MasterCard
Card Number _____
Expiration Date_____
Signature: _____

Please send your order form and prepayment made payable to:

**Cadmus Reprints**
**P.O. Box 751903**
**Charlotte, NC 28275-1903**

***Note: Do not send express packages to this location, PO Box.***
*FEIN #:541274108*

## Invoice or Credit Card Information

**Invoice Address Please Print Clearly**
**Please complete Invoice address as it appears on credit card statement**

Name _____
Institution _____
Department _____
Street _____
City _____ State _____ Zip _____
Country _____
Phone _____ Fax _____
E-mail Address _____

**Cadmus will process credit cards and *Cadmus Journal Services* will appear on the credit card statement.**

***If you don't mail your order form, you may fax it to 410-820-9765 with your credit card information.***

Signature _____ Date _____
Signature is required. By signing this form, the author agrees to accept the responsibility for the payment of reprints and/or all charges described in this document.

RB-9/22/06

# RadioGraphics 2007

## Black and White Reprint Prices

| Domestic (USA only) | | | | | | |
|---|---|---|---|---|---|---|
| # of Pages | 50 | 100 | 200 | 300 | 400 | 500 |
| 1-4 | $213 | $228 | $260 | $278 | $295 | $313 |
| 5-8 | $338 | $373 | $420 | $453 | $495 | $530 |
| 9-12 | $450 | $500 | $575 | $635 | $693 | $755 |
| 13-16 | $555 | $623 | $728 | $805 | $888 | $965 |
| 17-20 | $673 | $753 | $883 | $990 | $1,085 | $1,185 |
| 21-24 | $785 | $880 | $1,040 | $1,165 | $1,285 | $1,413 |
| 25-28 | $895 | $1,010 | $1,208 | $1,350 | $1,498 | $1,638 |
| 29-32 | $1,008 | $1,143 | $1,363 | $1,525 | $1,698 | $1,865 |
| Covers | $95 | $118 | $218 | $320 | $428 | $530 |

| International (includes Canada and Mexico) | | | | | | |
|---|---|---|---|---|---|---|
| # of Pages | 50 | 100 | 200 | 300 | 400 | 500 |
| 1-4 | $263 | $275 | $330 | $385 | $430 | $485 |
| 5-8 | $415 | $443 | $555 | $650 | $753 | $850 |
| 9-12 | $563 | $608 | $773 | $930 | $1,070 | $1,228 |
| 13-16 | $698 | $760 | $988 | $1,185 | $1,388 | $1,585 |
| 17-20 | $848 | $925 | $1,203 | $1,463 | $1,705 | $1,950 |
| 21-24 | $985 | $1,080 | $1,420 | $1,725 | $2,025 | $2,325 |
| 25-28 | $1,135 | $1,248 | $1,640 | $1,990 | $2,350 | $2,698 |
| 29-32 | $1,273 | $1,403 | $1,863 | $2,265 | $2,673 | $3,075 |
| Covers | $148 | $168 | $308 | $463 | $615 | $768 |

Minimum order is 50 copies. For orders larger than 500 copies, please consult Cadmus Reprints at 800-407-9190.

## Reprint Cover

Cover prices are listed above. The cover will include the publication title, article title, and author name in black.

## Shipping

Shipping costs are included in the reprint prices. Domestic orders are shipped via UPS Ground service. Foreign orders are shipped via a proof of delivery air service.

## Multiple Shipments

Orders can be shipped to more than one location. Please be aware that it will cost $32 for each additional location.

## Delivery

Your order will be shipped within 2 weeks of the journal print date. Allow extra time for delivery.

## Color Reprint Prices

| Domestic (USA only) | | | | | | |
|---|---|---|---|---|---|---|
| # of Pages | 50 | 100 | 200 | 300 | 400 | 500 |
| 1-4 | $218 | $233 | $343 | $460 | $579 | $697 |
| 5-8 | $343 | $388 | $584 | $825 | $1,069 | $1,311 |
| 9-12 | $471 | $503 | $828 | $1,196 | $1,563 | $1,935 |
| 13-16 | $601 | $633 | $1,073 | $1,562 | $2,058 | $2,547 |
| 17-20 | $738 | $767 | $1,319 | $1,940 | $2,550 | $3,164 |
| 21-24 | $872 | $899 | $1,564 | $2,308 | $3,045 | $3,790 |
| 25-28 | $1,004 | $1,035 | $1,820 | $2,678 | $3,545 | $4,403 |
| 29-32 | $1,140 | $1,173 | $2,063 | $3,048 | $4,040 | $5,028 |
| Covers | $95 | $118 | $218 | $320 | $428 | $530 |

| International (includes Canada and Mexico)) | | | | | | |
|---|---|---|---|---|---|---|
| # of Pages | 50 | 100 | 200 | 300 | 400 | 500 |
| 1-4 | $268 | $280 | $412 | $568 | $715 | $871 |
| 5-8 | $419 | $457 | $720 | $1,022 | $1,328 | $1,633 |
| 9-12 | $583 | $610 | $1,025 | $1,492 | $1,941 | $2,407 |
| 13-16 | $742 | $770 | $1,333 | $1,943 | $2,556 | $3,167 |
| 17-20 | $913 | $941 | $1,641 | $2,412 | $3,169 | $3,929 |
| 21-24 | $1,072 | $1,100 | $1,946 | $2,867 | $3,785 | $4,703 |
| 25-28 | $1,246 | $1,274 | $2,254 | $3,318 | $4,398 | $5,463 |
| 29-32 | $1,405 | $1,433 | $2,561 | $3,788 | $5,014 | $6,237 |
| Covers | $148 | $168 | $308 | $463 | $615 | $768 |

## Tax Due

Residents of Virginia, Maryland, Pennsylvania, and the District of Columbia are required to add the appropriate sales tax to each reprint order. For orders shipped to Canada, please add 7% Canadian GST unless exemption is claimed.

## Ordering

Reprint order forms and purchase order or prepayment is required to process your order. Please reference journal name and reprint number or manuscript number on any correspondence. You may use the reverse side of this form as a proforma invoice. Please return your order form and prepayment to:

**Cadmus Reprints**
P.O. Box 751903
Charlotte, NC 28275-1903

***Note: Do not send express packages to this location, PO Box.***
*FEIN #:541274108*

**Please direct all inquiries to:**

***Rose A. Baynard***
800-407-9190 (toll free number)
410-819-3966 (direct number)
410-820-9765 (FAX number)
baynardr@cadmus.com (e-mail)

**Reprint Order Forms and purchase order or prepayments must be received 72 hours after receipt of form.**